PARAMETERIZATION AND MICROMETEOROLOGICAL MEASUREMENT OF AIR–SEA GAS TRANSFER

C. W. FAIRALL
NOAA Environmental Technology Laboratory, Boulder, CO 80303, U.S.A.

J. E. HARE
CIRES, U. of Colorado, Boulder, CO 80303, U.S.A.

J. B. EDSON and W. MCGILLIS
Woods Hole Oceanographic Institution, Woods Hole, MA 02543, U.S.A.

(Received in final form 22 November 1999)

Abstract. Because of the combination of small concentrations and/or small fluxes, the determination of air–sea gas fluxes presents unusual measurement difficulties. Direct measurements (i.e., eddy correlation) of the fluxes are rarely attempted. In the last decade, there has been an intense scientific effort to improve measurement techniques and to place bulk parameterizations of gas transfer on firmer theoretical grounds. Oceanic tracer experiments, near-surface mean concentration profiles, eddy accumulation, and direct eddy covariance methods have all been used. Theoretical efforts have focused primarily in the realm of characterizing the transfer properties of the oceanic molecular sublayer. Recent major field efforts organized by the U.S.A. (GASEX-98) and the European Union (ASGAMAGE) have yielded atmospheric-derived results much closer to those from oceanographic methods. In this paper, we review the physical basis of a bulk-to-bulk gas transfer parameterization that is generalized for solubility and Schmidt number. We also discuss various aspects of recent sensor and technique developments used for direct measurements and demonstrate experimental progress with results from ASGAMAGE and GASEX-98. It is clear that sensor noise, sensitivity, and cross talk with other species and even ship motion corrections still need improvement for accurate measurements of trace gas exchange over the ocean. Significant work remains to resolve issues associated with the effects of waves, bubbles, and surface films.

Keywords: Gas flux, Carbon dioxide, Air–sea interaction, Diffusion sublayer, Turbulent transport.

1. Introduction

Air–sea fluxes of trace gases are of interest in atmospheric and oceanic pollution, biology, chemistry, and climate. For example, assessments of future human-induced global warming are critically dependent on quantifying the role of the oceans in the uptake of CO_2 and parameterizing the processes in global climate models. Traditional micrometeorological experimental and scaling theory methods have been quite successful in characterizing the transfer of momentum, sensible heat, and latent heat over both land and water (Panofsky and Dutton, 1984; Smith et al., 1996), and considerable advances have been made in their parametric representation in numerical models. Such methods have also had widespread application to

Boundary-Layer Meteorology **96:** 63–105, 2000.

the transfer of trace gases over land and vegetation, although a lack of fast-response sensors and small signal levels have precluded the use of the direct eddy covariance technique for many species of interest (Businger, 1986). This has led to investigation of a variety of alternative measurement methods (Businger and Delaney, 1990), although the eddy covariance method is still considered the standard.

Because of the low aerodynamic roughness of the ocean, measurement and characterization of air–sea gas transfer has presented a host of new problems. Initially, direct measurements (i.e., eddy correlation) of the fluxes over the open ocean were not technically feasible. Instead, fluxes were most commonly estimated via a bulk relationship

$$F_t = V_t \Delta X, \tag{1}$$

where V_t is a transfer velocity and ΔX the effective sea-air concentration difference. This is the same form of parameterization used in numerical models. Wind-water tunnel studies (Liss and Merlivat, 1986) and isotopic distributions (Broecker and Peng, 1974) were first used to estimate the transfer velocity. However, early attempts to verify these results using micrometeorological methods revealed one to two orders of magnitude disagreement and triggered a controversy (Broecker et al., 1986; Smith and Jones, 1986; Wesely, 1986) that is still unresolved. For example, a recent 'consensus' representation shown in Figure 1 (Wanninkhof, 1992) of V_t used no micrometeorological data sources. Note the disparity between these empirical parameterizations and the more recent micrometeorological result of Smith et al. (1991).

Another aspect of the air–sea flux problem is the need for parameterizations with a deep connection to the basic physics. Global applications and the demands for extreme accuracy are proving too much for simple representations of stress and thermodynamic fluxes through one or two empirical constants. Considerations of the matching of molecular sublayer and turbulent diffusion processes has led to improved transfer coefficients for heat and moisture (Brutsaert, 1982; Clayson et al., 1996; Liu et al., 1979), although the improvement turns out to be modest compared to constant coefficients. Air–sea gas transfer is entirely different. With the vast dispersion in diffusional and solubility properties for the many chemical species of interest, it is clear that a purely empirical approach will require far too much field work because we will be unable to apply the results from one gas to another gas. If we can include a sufficient physical basis, then the transfer properties of, say, heat, CO_2, and radon can be handled by a single parameterization (e.g., see Soloviev and Schluessel, 1994). Furthermore, information gained through analysis of an easily studied variable (e.g., heat/temperature) can be applied to a variable that is experimentally less tractable (e.g., CO_2). The number of physical processes of relevance is, unfortunately, formidable (see summary by Coantic, 1980; or the volume by Jahne and Monahan, 1995).

Advancement in measurement technologies and a re-invigoration of interest in molecular/diffusional sublayer processes associated with the need for accur-

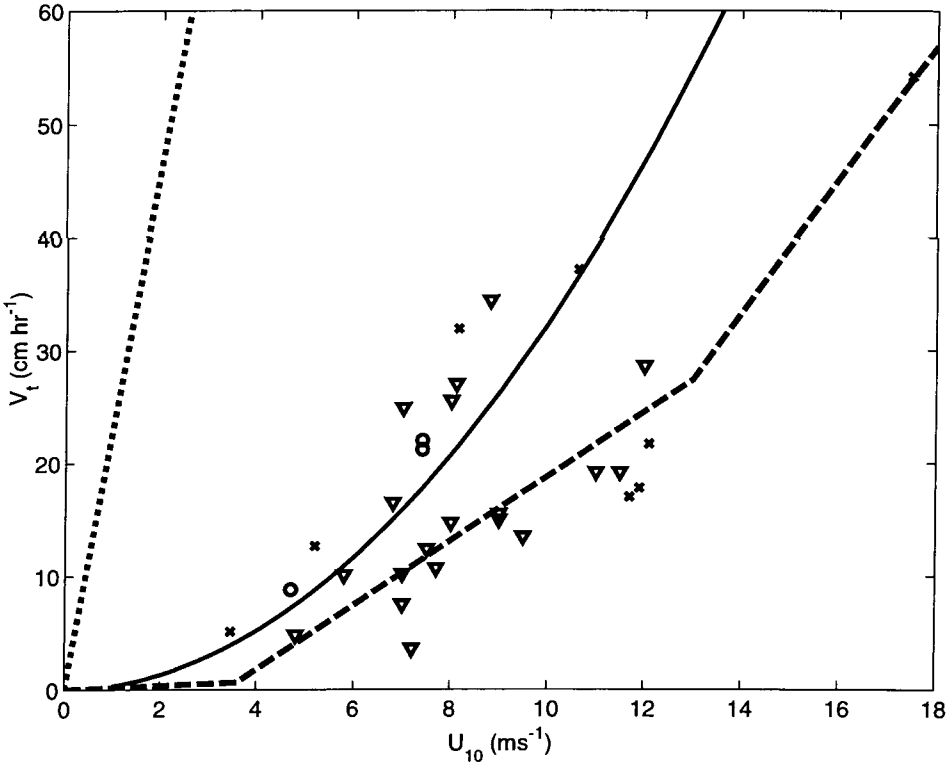

Figure 1. CO_2 transfer velocity at S_c = 600 versus 10-m wind speed. The dashed line is from laboratory studies (Liss and Merlivat, 1986); the solid line and the tracer-study points are from Wanninkhof (1992): ×, $^3He/SF_6$; triangles, ^{222}Rn; circles, $^{14}Carbon$. The dashed line is the early micrometeorological result from (Smith et al., 1991). The tracer studies are for long time scales (months to years).

ate models of oceanic near-surface temperature gradients in the last decade have stimulated strong programs of investigation of gas transfer processes in research laboratories around the world. The approach is to perform simultaneous measurements of gas transfer using a spectrum of atmospheric and oceanic techniques, with an emphasis on understanding the underlying physics. The philosophy is that not only must oceanic and micrometeorological measurements be consistent, but disagreements between various direct and indirect techniques must also be reconciled. This 'holistic' approach to the problem requires unusual levels of cooperation between disparate experimental groups but is considered by many to be necessary for credibility in atmospheric, oceanic, chemical, and physical scientific communities. Recent progress in these endeavors is the subject of this paper. Our purpose is to re-examine the theoretical basis of present parameterizations and to discuss various micrometeorological measurement issues so that we can place a perspective on new measurement programs (note, for a more complete review of physical and chemical aspects of trace gas transfer, see Asher and Wanninkhof, 1998a). After reviewing

standard turbulence scaling theory, we will summarize the components of bulk-to-bulk models of gas transfer; a discussion of micrometeorological measurement issues will be followed by some preliminary results from recent field programs.

2. Background

2.1. Flux definitions and Monin–Obukhov similarity

The conservation equation for the ensemble mean of a scalar quantity χ, denoted as X, under horizontally homogeneous conditions is (Businger, 1986)

$$\frac{\partial \mathrm{X}}{\partial t} + \mathbf{U} \cdot \nabla \mathrm{X} = -\frac{\partial(-D_\chi \partial \mathrm{X}/\partial z + \overline{x'\chi'})}{\partial z} + \overline{Q_\chi}, \tag{2}$$

where $\mathbf{U}$ is the wind vector, w is the vertical component D_χ the molecular diffusion coefficient, primes denote turbulent fluctuations, and Q_χ represents all source terms. The quantity of interest is the flux (sum of turbulent and molecular diffusive) enclosed in the parentheses; its value near the interface characterizes the air–sea transfer.

Monin–Obukhov Similarity Theory (MOST) is used to describe turbulent properties in the surface layer (Panofsky and Dutton, 1984); scaling parameters are defined in terms of the turbulent fluxes,

$$\chi_* = -\overline{(w'\chi')_s}/u_*, \tag{3}$$

where $\chi = u$, T, or q, and the s subscript denotes the surface value of the flux. MOST is based on the idea that in the surface layer, the dynamical variables can be scaled by combinations of these parameters plus the height, z, and that the dimensionless properties are then functions of $\zeta = z/L$, where

$$\zeta = \frac{\kappa g z}{T}(T_* + 0.61 T q_*)/u_*^2, \tag{4}$$

L is the Obukhov length, g is the acceleration of gravity, and κ is the von Kármán constant (0.4).

Details on MOST can be found in the texts referenced above, but a few examples are given here. The vertical gradient of the mean of some variable, X, can be represented by

$$\frac{\partial \mathrm{X}}{\partial z} = \frac{\chi_*}{\kappa z}\varphi_\chi(\zeta), \tag{5}$$

where φ_χ is the empirically determined dimensionless gradient function. We can integrate (5) to describe the profile (Panofsky, 1963; Paulson, 1970),

$$\mathrm{X}(z) - \mathrm{X}_s = \frac{\chi_*}{\kappa}[\ln(z/z_{0\chi}) - \Psi_\chi(\zeta)], \tag{6}$$

where $z_{0\chi}$ is the surface roughness length, which in this form is an unknown constant of integration. From (6) we can define transfer coefficients associated with the scaling parameters, χ_*

$$c_\chi^{1/2} = \chi_*/\Delta X = \kappa/[\ln(z/z_{0\chi}) - \Psi_\chi(\zeta)], \tag{7}$$

where c_d, c_T, and c_q are the transfer coefficients for velocity, temperature, and moisture scaling parameters.

2.2. Bulk flux representations

Standard micrometeorological *bulk* representations of the fluxes are based on (3) and (6)

$$\begin{aligned}\overline{w'\chi'} &= -u_*\chi_* = \frac{\kappa^2 S(\mathrm{X}_s - \mathrm{X}_r)}{[\ln(z_r/z_0) - \Psi_u(\zeta)][\ln(z_r/z_{0\chi}) - \Psi_\chi(\zeta)]} \\ &= C_\chi S(\mathrm{X}_s - \mathrm{X}_r),\end{aligned} \tag{8}$$

where the transfer coefficients for stress and sensible and latent heat are denoted by C_χ and

$$C_\chi = c_\chi^{1/2} c_d^{1/2}. \tag{9}$$

X_s is the mean variable value at the surface, and X_r is the value at some *reference* height z_r. Note that in this convention, X = U_x, U_y are the horizontal wind components relative to the ocean surface and S is the average value of the wind speed relative to the mean sea surface at z_r. Measurements of winds, temperature, humidity, and sea surface temperature are used with (8); the solution is usually found iteratively (Geernaert, 1990). Note that (8) implies that $V_{t\chi} = C_\chi S$; thus, air–sea gas transfer will tend to be proportional to wind speed.

The neutral transfer coefficients are related to the roughness lengths, which are defined as the height where the extrapolation of the logarithmic portion of the variable profile intersects the surface value

$$c_{xn}^{1/2} = \kappa/\ln(z_r/z_{0x}). \tag{10}$$

where the subscript n denotes neutral stability ($\zeta = 0$); (10) follows from (7) with $\Psi(0) = 0$. The velocity roughness length, z_0, is often crudely related to the physical roughness of the surface (see Panofsky and Dutton, 1984, p. 123), but the scalar roughness lengths are more complicated (Garratt, 1992; Kraus and Businger, 1994). This is discussed in more detail in Sections 3–4. Over the ocean, Smith (1988) has expressed the roughness length as the sum of a smooth flow limit and a Charnock-type dependence,

$$z_0 = \frac{A_l u_*^2}{g} + \frac{0.11\nu}{u_*}, \tag{11}$$

where A_l is the Charnock constant (between 0.011 and 0.018 for the open ocean) and ν is the kinematic viscosity.

2.3. The low wind speed limit

Another topic of interest is the form of the transfer coefficients in the limit of low wind speed. Note that in (8), the parameter S is, in fact, the average value of the wind speed, not the magnitude of the mean wind vector. Godfrey and Beljaars (1991) have expressed S as

$$S^2 = U_x^2 + U_y^2 + W_g^2 = U^2 + W_g^2, \tag{12}$$

where U_x and U_y are the mean wind components (as in Section 2.2), and W_g is proportional to the convective scaling velocity, as follows

$$W_g = B_e W_* = B_e \left(\frac{g}{T} \overline{w'\theta_v'} z_i \right)^{1/3}, \tag{13}$$

where B_e is an empirical constant of the order of unity, θ_v the virtual potential temperature, and z_i the depth of the convective boundary layer; B_e depends on the temporal/spatial scale used to compute the averages (Fairall et al., 1996a). In this paper we emphasize the application of (8) and (13) to time averages of point measurements. Similar expressions may be used in numerical models (Beljaars, 1994; Zulauf and Krueger, 1997), however the use of gridscale/time averages (Tong et al., 1998; Vickers and Esbensen, 1998) may require incorporation of more physical processes.

3. Bulk Parameterization Theory

In the representation of bulk flux relationships, the transfer coefficients (transfer velocity, drag coefficient, or roughness lengths) can be considered as empirical quantities that are directly determined by measurement. As such, they parameterize the entire transfer process from the interface to the measurement height in the turbulent surface layer. However, these parameterizations can be moved one level deeper into the physics by considering the well-known behaviour of turbulent diffusion in the surface layer. We begin by rewriting (2),

$$\frac{\partial \mathrm{X}}{\partial t} + \mathbf{U} \cdot \nabla \mathrm{X} = -\frac{\partial}{\partial z} \left(-(D_\chi + K_t) \frac{\partial \mathrm{X}}{\partial z} + F_{q\chi} \right), \tag{14}$$

where K_t is the turbulent diffusion coefficient, and we have replaced the point source term, Q_χ, with its vertical integral to express it as a flux, $F_{q\chi}$.

3.1. THE DIFFUSION EQUATION AND PROFILE RELATIONSHIPS

In the surface layer over the ocean, we can neglect the terms on the left side of (14) (horizontal homogeneity and stationarity) and vertically integrate the remainder,

$$-(D_\chi + K_t)\frac{\partial \mathrm{X}}{\partial z} + F_{q\chi} = \text{Constant} = F_{\chi_s} + F_{q\chi_s}, \tag{15}$$

where the subscript 's' denotes the values at the interface (although any height can be used since the sum is a constant) and the F_χ term refers to the total (molecular plus turbulent diffusive) flux of the quantity χ. We can re-arrange (15) and integrate in z to reference height, z_r, to obtain a general expression relating the bulk surface-to-fluid difference to the flux:

$$\Delta \mathrm{X} = \mathrm{X}_s - \mathrm{X}_r = \int_0^{z_r} \frac{F_{\chi_s} + [F_{q\chi_s} - F_{q\chi}(z)]}{D_\chi + K_t(z)}\,\mathrm{d}z. \tag{16}$$

In the absence of a significant source (say, for CO_2), $F_{q\chi}$ terms cancel and the constant becomes the flux of the quantity of interest, F_χ (which is independent of z in this case)

$$\Delta \mathrm{X} = F_{\chi_s} \int_0^{z_r} \frac{\mathrm{d}z}{D_\chi + K_t(z)} = \frac{F_{\chi_s}}{V_t}. \tag{17}$$

In the case where χ represents temperature, the source term is radiative flux divergence and release of latent heat from water phase transitions. Thus, on the atmospheric side of the interface Q_χ is negligible so (17) applies with $F_{\chi_s} = H_s/(\rho_a c_{pa})$, where H_s is the sensible heat flux, and ρ and c_p are the density and specific heat of the fluid, with subscripts a and w denoting air and water. On the oceanic side, we must use (16) and account for cooling realized essentially at the interface (the sum of sensible and latent heat plus the net longwave radiative cooling) and the profile of solar radiative flux in the water column. See Fairall et al. (1996b) for a discussion of the oceanic temperature profile in the molecular sublayer (cool skin) and the turbulent boundary layer (diurnal warm layer).

3.2. THE TURBULENT DIFFUSION COEFFICIENT

Solutions to (16) and (17) require a specification of the behaviour of the turbulent diffusion coefficient. From MOST, we can use (5) to express the turbulent diffusion coefficient as

$$K_t = \kappa z u_* / \phi_\chi(z/L). \tag{18}$$

However, this ignores the suppression (dissipation) of small-scale turbulent velocity fluctuations by viscosity, which occurs at the scale, δ_u, proportional to the Kolmogorov microscale

$$\delta_u = \lambda_1 \delta_k = \lambda_1 \nu / u_*, \tag{19}$$

where λ_1 is a coefficient. For flow over smooth surfaces, we can modify the K_t profile to account for this reduction in turbulent diffusion

$$K_t = \kappa z u_* / \left[1 + \left(\frac{\delta_u}{z}\right)^m\right], \tag{20}$$

where we have neglected (for the moment) the MOST stability term and m is some power. Using an alternate approach based on continuity near an interface, Hasse and Liss (1980) present arguments that $m = 2$ for a smooth surface and recommend a specific form due to Reichardt (1951). Near the surface, (20) implies that K_t will go as z^{m+1}.

3.3. THE SCALAR MOLECULAR SUBLAYER THICKNESS

If we define the molecular sublayer for the quantity χ as the region near the surface ($z < \delta_\chi$) where D_χ exceeds K_t, then (19) and (20) imply that

$$\delta_\chi = \delta_u (\lambda_1 \kappa S_c)^{-\frac{1}{m+1}} = \lambda_2 \frac{\nu}{u_*} S_c^{-\frac{1}{m+1}}, \tag{21}$$

where $S_c = \nu / D_\chi$ is the Schmidt number. The smooth flow regime is expected to have $m = 2$, which leads to δ_χ proportional to $S_c^{-1/3}$. Surface renewal theory (see discussion in the next section) leads to a $S_c^{-1/2}$ dependence, which corresponds to $m = 1$.

4. Bulk Layer Models

4.1. THE SIMPLE TWO-LAYER MODEL

We can use (17) to create approximate bulk relationships by separating the integral into molecular and turbulent sublayer components

$$\Delta X / F_{\chi s} = \int_0^{\delta_\chi} \frac{dz}{D_\chi + \kappa u_* z^{m+1} / \delta_u^m} + \int_{\delta_\chi}^{z_r} \frac{dz}{\kappa u_* z}, \tag{22}$$

where we have assumed $\delta_\chi < \delta_u$. The scalar molecular sublayer integral can be written in the form

$$k_\chi^{-1} = \frac{\delta_u}{D_\chi (\kappa \lambda_1 S_c)^{\frac{1}{m+1}}} \int_0^1 \frac{dz'}{1 + (z')^{m+1}} \approx \Lambda S_c^{\frac{m}{m+1}} / u_*, \tag{23}$$

where Λ is a coefficient that is related to other coefficients we have introduced (or it may be viewed as an empirical coefficient itself) and we have approximated the integral by ignoring the $(z')^{m+1}$ term. Thus, the transfer velocity is given by

$$1/V_t = 1/k_\chi + \ln(z_r/\delta_\chi)\kappa u_*, \tag{24}$$

and its determination requires a specification of u_*, k_χ, and δ_χ. In micrometeorology, the individual terms in (24) are often considered as flow resistances and V_t^{-1} the total flow resistance resulting from two resistances in series.

Note that the two-layer approximation is not always required. For $m = 1$ or $m = 2$, (17) and (20) can be integrated to give an analytical form for the profile. For example, for $m = 1$ we obtain

$$\frac{\Delta X}{F_{\chi_s}} = \frac{1}{2c}\log(G/a) + \frac{2(\delta_u - b/2c)}{d}[\tan^{-1}[(b+2cz)/d] - \tan^{-1}(b/d)], \quad (25)$$

where $G = a + bz + cz^2$, $a = D_\chi \delta_u$, $b = D_\chi$, $c = \kappa u_*$, and $d = (4D_\chi \delta_u \kappa u_* - D_\chi^2)^{1/2}$. The first term gives the required logarithmic dependence for large z, while the second term describes the molecular sublayer part. For $S_c \gg 1$ and $z \gg \delta_\chi$, we can expand (25) and obtain

$$\frac{\Delta X(z_r)}{F_{\chi_s}} = \frac{1}{\kappa u_*}\ln\left[\frac{z}{\delta_u(\lambda_1 \kappa S_c)^{-1/2}}\right] + \frac{\pi}{2}(\lambda_1 S_c/\kappa)^{1/2}/u_*. \quad (26)$$

The first term corresponds to the log-term in (24) where δ_χ comes from (21); the second term in (25) gives,

$$1/k_\chi = \frac{\pi}{2}\sqrt{\lambda_1/\kappa}\, S_c^{1/2}/u_*. \quad (27)$$

From (26) we can see that if we had chosen δ_u as the layer transition in (22) and (23), then (24) would take the form

$$1/V_t = 1/k'_\chi + \ln(z_r/\delta_u)/\kappa u_*, \quad (28)$$

where

$$1/k'_\chi = 1/k_\chi + \frac{1}{\kappa u_*}\ln(\lambda_1 \kappa S_c)^{1/2}. \quad (29)$$

The velocity sublayer resistance is greater in this case because it is over a deeper layer ($\delta_u > \delta_\chi$).

While the analytical solution to (17) and (20) may be exact, its philosophical advantage over the approximate form of (22) is modest because it is derived from a representation of the turbulent diffusivity that is, itself, an approximation. Furthermore, the two-layer approach provides some conceptual insight, illustrates the scaling relationships between sublayer thickness and k_χ, and allows us to combine log profiles with alternative models of k_χ.

4.2. SMOOTH VERSUS ROUGH FLOW

Another complication occurs when considering rough flow. Profiles of X in the form given in (6) extrapolate to the surface value when $z = z_{0\chi}$. For velocity in smooth flow, the roughness length would be about $0.1\nu/u_*$. In rough flow, the corrugations of the surface affect z_0, so properties of the transfer are scaled by the roughness Reynolds number, R_r,

$$R_r = z_0 u_*/\nu. \tag{30}$$

In purely smooth flow, $R_r \approx 0.1$, and purely rough flow occurs for $R_r > 1$. In rough flow, the simple mathematical forms such as (20) are not expected to be valid at heights near the roughness elements. Also, δ_u becomes a property of the surface and is not described by (19). Over the ocean, there are further complications because the fluid is not in contact with a fixed boundary but another fluid with internal turbulent and wave-induced motions.

4.3. MATCHING THE TWO LAYERS

At this point we will select $m = 1$ obtained from surface renewal theory used with $\lambda_1 \approx \lambda_2 \approx \Lambda \approx 10$ (see Kraus and Businger, 1994; Soloviev and Schluessel, 1994), but the reader is cautioned that this selection is subjectively based on the popularity of this form rather than definitive experimental evidence. Note that while we have reached the forms of (23) and (24) through the diffusion equation, the surface renewal approach yields an exponential shape for the sublayer profile and a parameterization of k_χ based on temporal decay arguments (Liu et al., 1979). Thus, the shape of the K_t profile is not dealt with directly. In this approach, the total dimensionless change in X across the molecular sublayer is characterized by

$$\Delta_\chi = \Lambda S_c^{1/2} R_r^{1/4}, \tag{31}$$

and the transfer is characterized through the exponential profile,

$$\frac{\Delta \mathrm{X}(z) u_*}{F_{\chi s}} = \Delta_\chi \left[1 - \exp\left(-\frac{z u_*}{\nu} S_c/\Delta_\chi\right)\right]. \tag{32}$$

The one-quarter power dependence of Δ_χ on roughness Reynolds number has been verified in some wind-tunnel studies (Chamberlain, 1968; Mangarella et al., 1973) but not in others (Ocampo-Torres and Donelan, 1994) and the relevance of laboratory results to the open sea has often been questioned (Hasse, 1990). Liu et al. (1979) match the exponential and logarithmic sublayer profiles and their slopes for velocity, temperature, and humidity to yield values for δ_χ, k_χ, and the roughness lengths of temperature and humidity. Note that only a fraction of the total possible transfer resistance (Δ_χ) is realized. An example of a near-surface profile for a

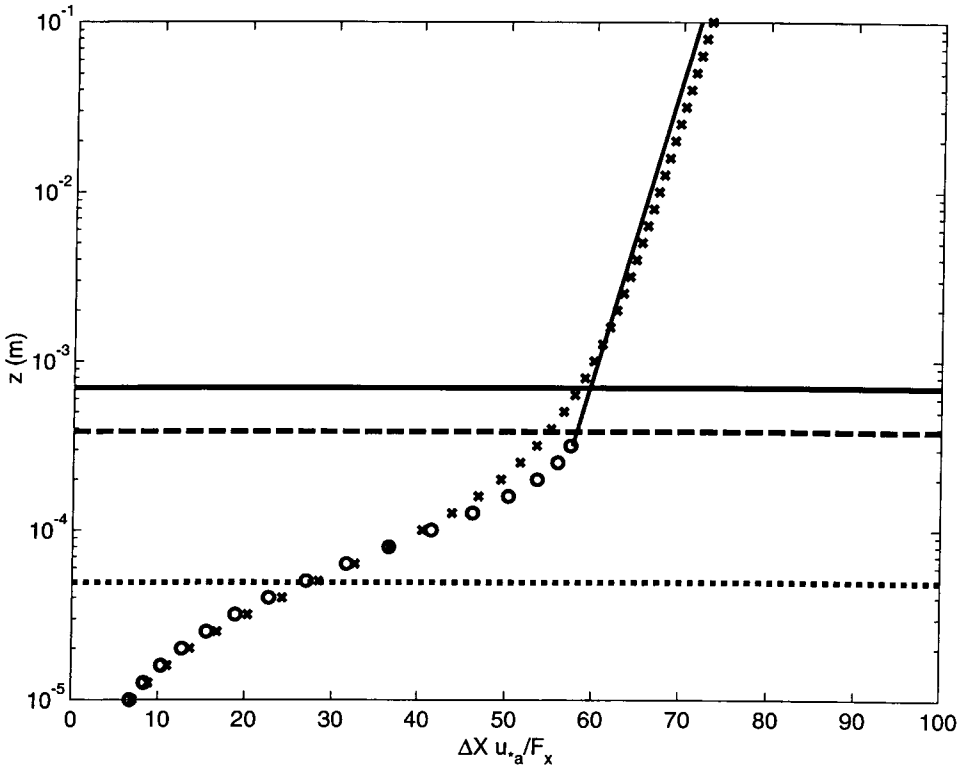

Figure 2. Normalized mean height profile of the scalar quantity X (referenced to zero at the surface) at $R_r = 1$. The circles and thin solid line use the matching method of Liu et al. (1979). The ×s are the analytical solution (25) with $\lambda_1 = 10$. The horizontal dashed line is at the Liu et al. (1979) matching point ($z = z_{mg}$); the horizontal dotted line is at δ_χ (the point where $D_\chi = K_t$) for the analytical model; the horizontal solid line is δ_u.

scalar with $S_c = 50$ and $R_r = 1.0$ (corresponding to an open ocean wind speed of about 7 m s^{-1}) is shown in Figure 2. Both Liu et al. (1979) and the analytical form from (25) are shown for comparison. In this example, about 72% of the total normalized change (65 for the molecular sublayer from a total of 90 to 10 m) from the surface to 10 m is realized in the molecular sublayer (the first half-mm). For $S_c = 1$, these same numbers are 8 out of 30 (27%), and for $S_c = 650$, they are 240 out of 270 (89%). For the particular case shown in Figure 2, there is a difference in the Liu et al. (1979) and (22) formulations, although this can be eliminated by adjusting the value for λ_1. These are the result of minor differences in the total (molecular plus turbulent) diffusivity profiles (Figure 3).

Brutsaert (1982) and Clayson et al. (1996) use surface renewal parameterizations of k'_χ similar to (25), but they do not attempt to match profile slopes; instead, they simply set $u_*/k'_\chi = \Delta_\chi$. This is tantamount to assuming that the maximum possible molecular sublayer flow transfer resistance is realized, an approximation that becomes more accurate as the Schmidt number increases.

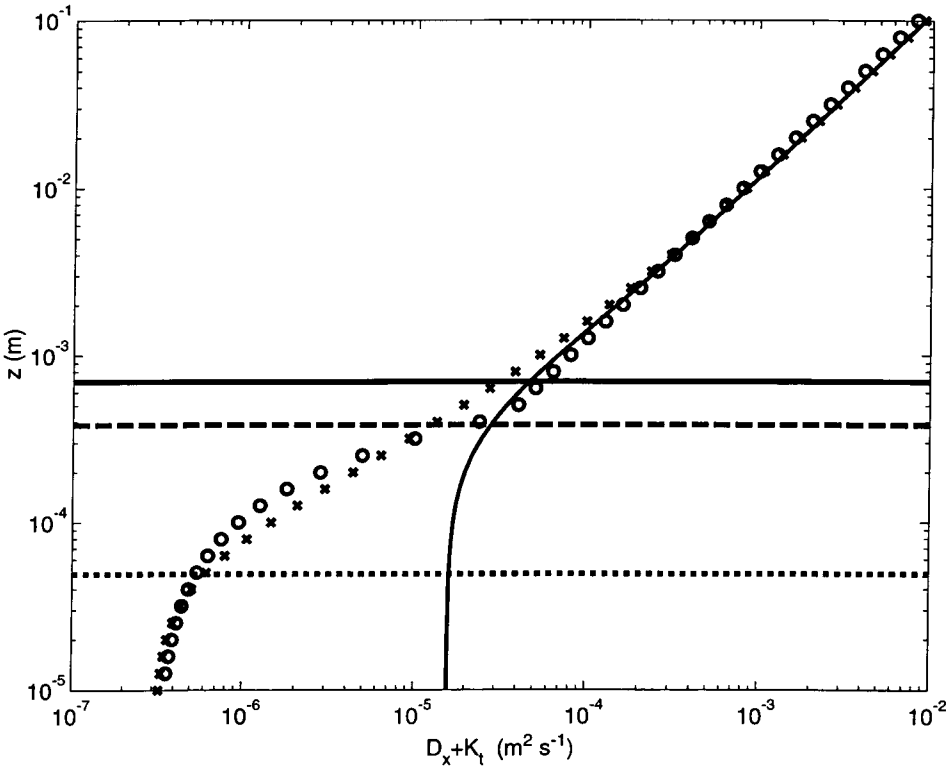

Figure 3. Profiles of the total diffusion coefficient (molecular plus turbulent) for $S_c = 50$: ×, (20) with $m = 1$ and $\lambda_1 = 10$; circles, form obtained by taking vertical derivative of the Liu et al. (1979) matched profile. The solid line is (20) with $S_c = 1$ (expected profile for velocity).

4.4. Relationship to roughness lengths

Matching of the molecular and turbulent sublayer profiles leads to a relation between sublayer thickness and the scalar roughness length. In the Liu et al. (1979) approach, the scalar roughness length follows from the matching of the two profile types,

$$z_{0\chi} = z_{m\chi} \exp(-\kappa u_*/k'_x), \tag{33}$$

where $z_{m\chi}$ is the matching height and u_*/k'_χ is obtained from (32). Note we use k'_χ because the Liu et al. (1979) matching height is near δ_u. In the Clayson et al. (1996) approach, the sum of the two sublayer parts is matched to the logarithmic profile in the turbulent sublayer as per (28) to give values for a value for V_t. From (8), (10), and (28), we can see that the matching condition is

$$u_*/k'_\chi + \ln(z_r/\delta_u)/\kappa = \ln(z_r/z_{0\chi})/\kappa. \tag{34}$$

This equation yields a relationship for the scalar roughness length

$$z_{0\chi} = \delta_\chi \exp(-\kappa u_*/k_\chi) = \delta_u \exp(-\kappa u_*/k'_\chi). \tag{35}$$

The form given in (35) relies on a specification of the velocity sublayer thickness. Note that k_χ and δ_χ may be used instead. However, the first log term can be expanded to eliminate an explicit specification of δ_χ other than the assumption that it is proportional to δ_u and scales as $S_c^{-1/2}$,

$$\begin{aligned}\ln(z_r/\delta_x)/\kappa &= \ln(z_r/z_0)/\kappa - \ln(\delta_u/z_0)/\kappa + \ln(\delta_u/\delta_x)/\kappa \\ &= c_d^{-1/2} - U_\delta/u_* + \ln[(\lambda_1\kappa Sc)^{1/2}]\kappa. \end{aligned} \tag{36}$$

This approach is particularly useful on the atmospheric side of the interface, where the velocity roughness length and drag coefficient are well-known and U_δ/u_* is on the order of 5 (Brutsaert, 1982). Thus, (34) and (36) yield a specification of scalar roughness length that can be used directly in (8),

$$z_{0\chi} = z_0 \exp[-\kappa(u_*/k'_\chi - 5)] = z_0(\lambda_1\kappa S_c)^{1/2} \exp[-\kappa(u_*/k_\chi - 5)]. \tag{37}$$

On the ocean side of the interface, (37) does not gain us much because knowledge of the velocity roughness in the water is almost non-existent (although it is usually assumed to be the same as the air-side roughness). The large orbital velocities of surface waves make direct measurements of z_0 and U_δ very difficult.

It is interesting to contrast the variety of possible scalar roughness length representations for a quantity that is well determined. In Figure 4, we illustrate neutral moisture transfer coefficients in the atmosphere as a function of 10-m wind speed using a specification of z_0 from (11) and $S_c = 0.6$. The circles are values obtained using (21) and k_χ from (23) with $m = 1$ in (35); the dots use (37) with the k'_χ formulation of Soloviev and Schluessel (1994); the line uses (37) with the k'_χ formulation of Clayson et al. (1996); and the crosses use (33) from Liu et al. (1979) as slightly modified by Fairall et al. (1996a). In this wind speed range, C_{en} is close to 1.1×10^{-3}. For most of the wind speed range, these different representations are within about 10%, which is probably acceptable for most characterizations of gas transfer.

4.5. BUOYANCY EFFECTS

The effects of buoyancy on the profiles in the turbulent sublayer are straightforwardly described by the Ψ functions in (6); these are relevant when $z_r > |L|/10$. Note that in (23) and (32), k_χ scales with u_*, which becomes negligible when the vector-mean wind becomes small. In this limit, convection still drives mixing across the molecular sublayer. Soloviev and Schluessel (1994), Fairall et al. (1996b), and Clayson et al. (1996) have all developed parameterizations to account for this effect when dealing with the ocean sublayers. In the first two papers, arguments about the buoyancy effects on the rate of dissipation of turbulent kinetic energy (see Section 6.1) are used to modify k_χ

$$u_*/k_\chi = \Lambda S_c^{1/2} R_r^{1/4}/\varphi(R_i/R_{ic}), \tag{38}$$

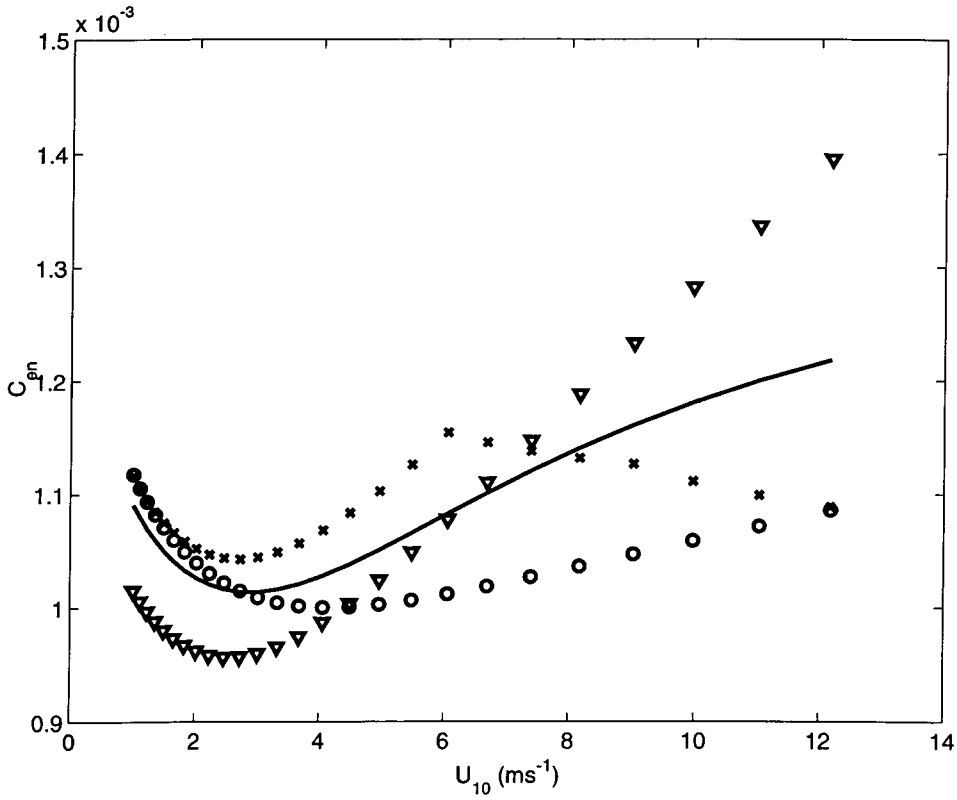

Figure 4. Neutral 10-m moisture transfer coefficient versus wind speed using four different representations of molecular sublayer processes as scalar roughness length: circles, (35) with $m = 1$; triangles, (37) with k'_χ from Soloviev and Schluessel (1994); line, (37) with $k'_\chi = u_*/\Delta_\chi$; and $\times$, from Fairall et al. (1996a).

where φ is an empirical function, R_i the molecular sublayer Richardson number, and R_{ic} a coefficient (on the order of 1.5×10^{-4}) that sets the threshold for buoyancy effects. The buoyancy flux, F_b, is used in the formulation of Richardson number

$$R_i = F_b \nu / u_*^4. \tag{39}$$

In unstable conditions, F_b will be nonzero as wind speed approaches zero and the product $u_* \varphi$ will approach a form proportional to $F_b^{1/4}$. Clayson et al. (1996) did something similar, except they use φ to combine shear-driven and buoyancy-driven surface renewal time scales. The present forms have been tuned to agree with measurements of the oceanic cool skin. Note, that these will lead to a finite gas transfer even at zero vector-mean winds.

4.6. SURFACTANT EFFECTS

The ocean is a dilute biological soup and it is known that organic materials can affect the surface viscoelasticity, surface tension and other variables affecting air–sea exchange (see Frew, 1997, for a review of this subject). The effects include the reduction of the length and velocity scales of the near-surface turbulence in the ocean, damping of high frequency waves, inhibition of wave growth, and enhancement of wave energy dissipation. Laboratory investigations have clearly demonstrated surfactant effects on gas transfer velocities. Considerable progress has been made in biological and film sampling techniques for the ocean (Hunter, 1997), but efforts to link variations in gas exchange properties directly to surfactants require accurate, high time resolution measurements of gas transfer. We make no attempt to offer improvements in transfer parameterizations based on oceanic surfactant properties, but merely alert the reader that we are neglecting a physical process that may be significant in some conditions.

5. Two-Fluid Matching

5.1. WATER–AIR FLUX EXPRESSION

The next step in our development is the computation of air–sea flux given a specification of bulk concentrations (i.e., well away from the interface and the molecular transfer region) in the air and water. If the source terms are negligible, then we may characterize the flux in each fluid using our simple transfer velocity equation (Liss, 1973)

$$F_{s\chi} = V_{ta}(\mathrm{X}_{sa} - \mathrm{X}_{ra});\ F_{s\chi} = V_{tw}(\mathrm{X}_{rw} - \mathrm{X}_{sw}), \tag{40}$$

where the subscripts a and w refer to air and water, s and r refer to interface and bulk, and we have defined the flux positive upward. We now divide by the flux and isolate the interfacial values,

$$F_{s\chi}/V_{ta} + \mathrm{X}_{ra} = \mathrm{X}_{sa};\ F_{s\chi}/V_{tw} + \mathrm{X}_{rw} = -\mathrm{X}_{sw}. \tag{41}$$

5.2. SOLUBILITY

If temperature is the variable of interest, then we require continuity at the interface ($\mathrm{X}_{sa} = \mathrm{X}_{sw}$). For water vapour, the interfacial value appropriate for the air side transfer is the water vapour pressure, which is a function of temperature and salinity (see Chapter 2 in Kraus and Businger, 1994). For trace gases in the atmosphere, the effective vapour pressure is proportional to the concentration in the water (Liss, 1973):

$$\mathrm{X}_{sa} = \mathrm{X}_{sw}/\alpha, \tag{42}$$

where α is the dimensionless solubility. We can now eliminate the surface concentrations and solve for the flux in terms of the bulk concentrations

$$F_s = \frac{[\mathrm{X}_{rw} - \alpha \mathrm{X}_{ra}]}{V_{tw}^{-1} + \alpha V_{ta}^{-1}] } = \frac{[\mathrm{X}_{rw} - \alpha \mathrm{X}_{ra}]}{[R_{wm} + R_{wt} + \alpha R_{am} + \alpha R_{at}]}, \tag{43}$$

where the R terms represent the transfer variables expressed as flow resistances; χ subscripts have been made implicit to simplify the notation. The subscript m refers to the 'molecular' sublayer part (first term in Equation (24)) and the subscript t refers to the 'turbulent' layer part (second term in Equation (24)).

5.3. Final flux expressions

In open ocean conditions with a reasonable equilibrium wave state, we can assume continuity of the oceanic and atmospheric turbulent stress; thus,

$$u_{*w} = u_{*a}(\rho_a/\rho_w)^{1/2}. \tag{44}$$

We can now express the flux in a form that clearly shows the physical processes in each layer of both fluids

$$F_s = \frac{\alpha u_{*a}[\mathrm{X}_w/\alpha - \mathrm{X}_a]}{\sqrt{\rho_w/\rho_a}[1/k_w + \ln(z_w/\delta_w)/\kappa] + \alpha[1/k_a + \ln(z_a/\delta_a)/\kappa]}. \tag{45}$$

Carrying this one step further, we substitute (38) for k and write the flux in terms of the partial pressure difference, Δp_χ, for the relevant gas,

$$F_s = \frac{A u_{*a} \Delta p_\chi}{\sqrt{\rho_w/\rho_a}[h_w S_{cw}^{1/2} + \ln(z_w/\delta_w)/\kappa] + \alpha[h_a S_{ca}^{1/2} + C_d^{-1/2} - 5 + \ln(S_{ca})/(2\kappa)]}. \tag{46}$$

where the flux is expressed in mole $\mathrm{m}^{-2}\ \mathrm{s}^{-1}$, $A = 10^5\alpha/(R_{\mathrm{gas}}T)$ is the solubility in mole $\mathrm{m}^{-3}\ \mathrm{atm}^{-1}$, R_{gas} is the universal gas constant, and

$$h = \Lambda R_r^{1/4}/\varphi. \tag{47}$$

5.4. Discussion

We can use (46) to obtain insight into the importance of each fluid layer in resisting the transfer of gas molecules from the bulk water to the bulk atmosphere. In near-neutral conditions the term $C_d^{-1/2} - 5$ will be about 25 and the h terms will be about 10. Table I gives values of the Schmidt number for moisture, heat, and CO_2. We can see that heat, water vapour, and CO_2 will be transported with roughly equal

TABLE I

Nominal values for $S_c^{1/2}$ for selected variables in water and air.

	Water molecules	Heat	CO_2 molecules
Water	28	2.82	24.5
Air	0.77	0.80	0.91

efficiency in the atmosphere, but there will be significant differences in the water. Note also the factor of the square root of the ratio of densities (about 33) of water to air that multiplies the water transfer resistance, while there is a factor of solubility that multiplies the air transfer resistance. Air-side values for S_c tend to be near 1, so materials with solubilities less than 33 $S_{cw}^{1/2}$ will, all other factors being the same, encounter greater transfer resistance in the water. In the case of CO_2, α is about 1 and $S_c^{1/2}$ is nearly 30 times greater in the water. Thus, we can see that the molecular sublayer resistance for CO_2 in water is about 33×30 times greater than the sublayer resistance in the air (or about 300 times the *total* resistance in air).

As we discussed in Section 4, for S_c of 650 about 90% of the resistance in the single layer fluid occurs in the molecular sublayer. Thus, we expect that the transfer velocity or the dimensionless bulk transfer coefficient for CO_2 will be dominated by the water-side molecular sublayer resistance and will be about a factor of 300 smaller than that for moisture and heat in the atmosphere ($C_e \approx C_h \approx 1 \times 10^{-3}$)). These issues are discussed more eloquently and in more detail in the review by Jahne and Hausecker (1998). See, in particular, their Figure 2 where a number of gases of interest are displayed on a graph of S_{cw} and α.

6. High Wind Complications

As wind speed over the ocean increases, several physical factors increase the uncertainty (or are not even considered) in the simple parameterizations discussed in Section 5. At about 6–7 m s^{-1}, breaking waves appear on the ocean surface (O'Muircheartaigh and Monahan, 1986); they affect the velocity roughness and produce air bubbles in the upper ocean mixed layer. Conventional bulk transfer schemes tend to diverge as wind speeds exceed 10 m s^{-1} (Zeng et al., 1998) and the influence of sea spray on the heat and moisture transfer, while hotly debated (Andreas et al., 1995), may become significant as wind speed exceeds 20 m s^{-1} (Andreas, 1998).

Effects on bulk estimates of u_* or stability at high wind speeds are of some relevance, but in this section, we will concentrate on processes that more directly affect the gas transfer parameterizations. These include modification of turbulent

dissipation rates in the interfacial layer, enhanced turbulent transport in the ocean associated with waves, and enhanced gas exchange associated with bubbles and/or droplets.

6.1. NEAR-SURFACE TURBULENT DISSIPATION

Lamont and Scott (1970) related the molecular sublayer transfer velocity to the turbulent kinetic energy dissipation rate, ϵ, via

$$k_\chi = B S_c^{-1/2} (\epsilon \nu)^{1/4}, \tag{48}$$

where B is a constant. MOST 'law of the wall' scaling for the dissipation rate is

$$\epsilon = \frac{u_*^3}{\kappa z} \varphi_\epsilon (z/L). \tag{49}$$

If we set $z = \delta_u$, then (49) and (19) lead to forms such as (23). Several investigators have presented measurements that indicate oceanic ϵ is *enhanced* relative to (49) in the presence of breaking waves (Terray et al., 1996), while Edson et al. (1997) describe measurements that indicate a *reduction* in ϵ in air flow over waves In both cases, the departure from conventional scaling depends on wave age (wave phase speed, c_p, divided by atmospheric friction velocity), W_a. This is an example where small-scale laboratory simulations may not reproduce important physical processes at work in the open ocean. The dissimilarity of the effects of waves in water versus air breaks the similarity in the scaling expressions. Furthermore, Csanady (1990) described large-scale wave suppression of gas transfer due to microbreakers that reduces V_t at high wind speeds; this effect has been incorporated into the model of Soloviev and Schluessel (1994).

6.2. BREAKING WAVE TRANSPORT ENHANCEMENT

Monahan and Torgeresen (1991) discuss the issue of gas transfer through local ocean transport enhancement associated with breaking waves. In their approach, the oceanic molecular sublayer is bypassed and the turbulent sublayer is given a different exchange velocity, k_2, in the area of the whitecap. This wave-related exchange can be scaled in terms of the wave phase speed, wave height, and wavelength. This turns out to be equivalent to

$$k_2 = c_2 W_a u_{*w}, \tag{50}$$

where laboratory whitecap simulations give $c_2 \approx 0.03$; a typical open ocean value for W_a is around 25. Thus, the total resistance in the ocean, as expressed in (43), is replaced by an effective 'parallel' resistance,

$$(R_{wm} + R_{wt}) \rightarrow [(1 - f)/(R_{wm} + R_{wt}) + f k_2]^{-1}, \tag{51}$$

where $f = 3.8 \times 10^{-6}\ \mathrm{U}^{3.4}$ is a simple parameterization of the whitecap fraction.

6.3. BUBBLE-MEDIATED ENHANCEMENT

In the last decade, a great deal of research has been devoted to investigation of the bubble enhancement of gas transfer. The primary physical effects are the enhancement of the dissolving processes by transport of air bubbles to greater depth/pressure and the bypassing of the molecular sublayer bottleneck as bubbles reach the surface, break, and release gases. The subject matter is too vast to summarize here; we suggest Chapter 3 in Jahne and Monahan (1995) and the recent review by Asher and Wanninkhof (1998a). As an example of bubble treatment in gas flux parameterization, we offer one from Woolf (1997)

$$F_s = (V_{t0} + k_b)[X_{wr} - \alpha X_{ar}(1 + \Delta)], \tag{52}$$

where V_{t0} represents the non-bubble transfer such as from (45), k_b a bubble-associated transfer velocity, and Δ a bubble-associated enhancement of the gas concentration. Woolf (1997) gives an estimate of k_b

$$k_b = V f \alpha^{-1}[1 + (e\alpha S_c^{-1/2})^{-1/n}]^{-n}, \tag{53}$$

where $V = 6.8 \times 10^{-3}$ m s^{-1} characterizes the ventilation associated with whitecaps; for CO_2, e = 14 and n = 1.2. Recent alternate bubble treatments can be found in Keeling (1993) and Asher et al. (1996).

The behaviours of sample parameterizations including wave breaking (50) and bubble effects (52) are shown as a function of wind speed in Figure 5a for an air temperature of 20 °C with a nominal sea-air temperature difference of 1.5 °C and a relative humidity of 82%. The Wanninkhof (1992) curve and (44) with the Fairall et al. (1996b) version of k_w are shown for reference. The value of c_2 has been set at 0.0075 to fit the Wanninkhof curve, so there is little significance to the goodness of fit. In Figure 5b, we repeat the plot but with an air temperature of 0 °C and the disagreement is apparent; this shows the lack of physical consistency of the three parameterizations.

6.4. SEA-SPRAY DROPLET ENHANCEMENT

Gas transfer associated with evaporating sea spray droplets has received little attention. A number of issues must be considered. In strong winds, the mass mode of sea spray concentrations is about 50 μm radius; this is so small that the molecular sublayer bottleneck may not be a factor. Also, a droplet that has evaporated to its equilibrium size at 80% relative humidity is about half its original size at sea water salinity. Thus, its volume is about one eighth and its air–water concentration difference is about 8 times greater. Both of these factors suggest droplets will be orders of magnitude more efficient at transferring gas between air and seawater.

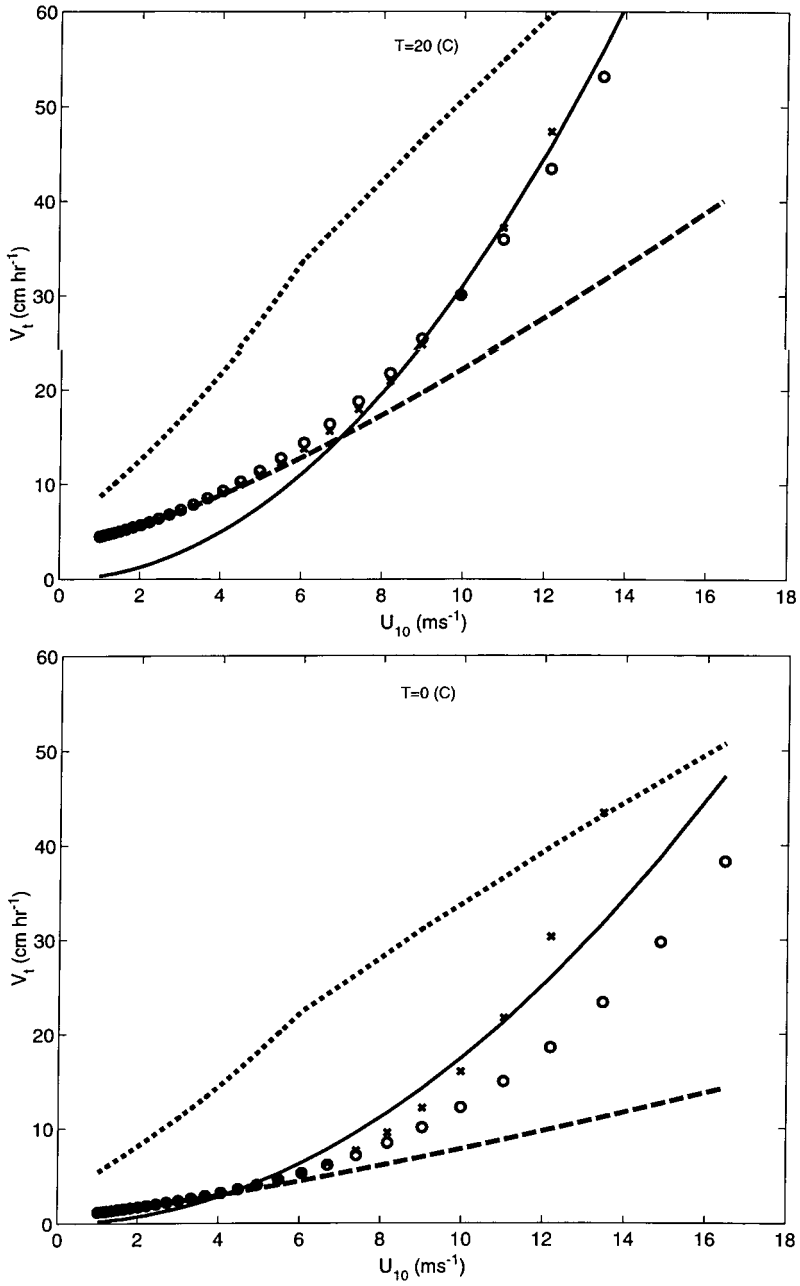

Figure 5. Sample parameterizations of CO_2 transfer velocity as a function of wind speed: (a, upper) air temperature = 20 °C and (b, lower) air temperature = 0 °C. The solid line is from Wanninkhof (1992), the dashed line (46), the × from (51) with $c_2 = 0.0075$, and the circles from (52). The dotted line is the Webb et al. (1980) mean vertical velocity for these conditions (see end of Subsection 7.3).

However, depending on the wind speed, droplets of a size exceeding a threshold characterized by their gravitational settling velocity over u_{*a} (Toba, 1965) tend to fall back into the ocean before reaching equilibrium size. Thus, considerations of suspension, evaporation, and gas transfer time scales are required (Andreas, 1992). The potential impact of sea spray on gas transfer is difficult to characterize, but it is interesting to consider a recent (Andreas and DeCosmo, 1999) estimate of the surface area of suspended sea spray droplets per unit area of sea surface as a function of wind speed, which indicates droplet surface area is 10% of 'flat ocean' area at a wind speed of 25 m s^{-1}. If droplets do have greatly enhanced transfer properties, then they will become important at these wind speeds. With the recent development of numerical models capable of dealing with most of the complex physics of the evaporating sea spray problem (Kepert and Fairall, 1999), the stage is set for an investigation of this issue.

7. Micrometeorological Measurement Issues

The great majority of credible estimates of gas transfer parameters to date have been made using laboratory simulations or oceanic tracer methods (Asher and Wanninkhof, 1998b). Laboratory methods can be done very accurately, but critical physical processes may not be included and their application to the ocean is open to interpretation. That is, if a certain wind-tunnel result is obtained, do we assume the result applies over the ocean at the same values of wind speed, u_{*a}, u_{*w}, R_r? Oceanic tracer methods include analysis of natural tracers such as ^{222}Rn, man-made but accidental tracers such as ^{14}C from testing of nuclear weapons, and deliberate tracers such as SF_6 and ^{3}He. The fundamental time scale of tracer methods varies from days to years, so it may be impossible to examine parametric dependencies such as stability or whitecap fraction that vary on much shorter time scales. Possible multiple Schmidt number dependencies of bubble-mediated exchange processes also introduce complexities to the tracer method (Asher and Wanninkhof, 1998a). Micrometeorological methods can yield results on time scales of roughly one hour. Also, both laboratory and tracer techniques are essentially budget methods in which the concentrations and/or their rates of change are used to infer the flux, whereas the covariance method is a direct measurement of the quantity of interest. For the remainder of this paper, we will focus on micrometeorological methods. The general methods have been discussed in detail in numerous sources (Businger, 1986; Kaimal and Finnigan, 1994; Kraus and Businger, 1994; Smith et al., 1996; Wyngaard, 1990), so we will emphasize aspects with main relevance to gas transfer.

The flux can be determined by measuring the time or space series of w' and χ' and computing their mean cross product; this is referred to as the 'covariance' or 'eddy-correlation' method. Besides the covariance method, there is a host of other indirect approaches based on applications of MOST to measured properties other

than the covariances. Note that these other methods yield estimates of the *surface* flux only, while the covariance method is general. This diversity of flux methods is primarily due to the historical difficulty, expense, and impracticality of making the direct covariance measurements for all variables of interest on the horizontal and temporal scales of interest. Measurements over the ocean involve the additional complication of platform motion (Fujitani, 1985), flow distortion by booms, other instruments, and the platform (Oost et al., 1994), and contamination by sea spray and salt particles (Schmitt et al., 1978). Fast-response sensors are still not available at the time of writing for a number of gas and particle species of interest, but the gradient and relaxed eddy accumulation (REA) methods use measurements of mean concentration difference (see below).

7.1. COVARIANCE METHODS

As discussed above, eddy correlation is essentially the standard upon which other indirect methods are based. In principle, once sensor calibration errors and other sources of error are removed and the sensors have adequate frequency response to resolve the relevant scales of turbulence (about 10 Hz), covariance computations represent an unbiased estimate of the true ensemble mean of interest at the height of the measurement (see Businger (1986) for a discussion of the difference between the flux at height z and the true surface flux caused by horizontal inhomgeneity, non-stationarity, and entrainment). From a practical point of view, we do not measure the actual ensemble average, but compute estimates from time/space series of data taken on towers, platforms, ships and aircraft.

$$F_\chi = \langle w'\chi' \rangle_T, \tag{54}$$

where the $\langle\,\rangle$ denote a time average of duration T. Note that this is, in fact, consistent with most modern numerical models, which represent fluxes, not as ensemble averages, but in terms of resolved ($\langle w \rangle \langle \chi \rangle$) and unresolved ($\langle w'\chi' \rangle$) components, although the relationship between point/time averages of most measurements and space/time averages in volume-average models has been studied very little (Tong et al., 1998; Vickers and Esbensen, 1998). This issue is also relevant in analysis of 'climate-scale' fluxes (Esbensen and Reynolds, 1981; Hanawa and Toba, 1987; Weare and Strub, 1982).

A particular eddy correlation measurement (say, a 1-h average) is considered to be an estimate of the true flux subject to some statistical sampling uncertainty (Wyngaard, 1973). For 1-h averages, this uncertainty is on the order of 20%, but is highly dependent on conditions. It is assumed that the effects of sampling error are random and, therefore, can be reduced by averaging a collection of flux values. The choice of averaging period is not arbitrary; Mahrt et al. (1996) discussed trade-offs between high-pass filtering of the time series, the time scale of the average computation, and nonstationarity of the data. High-pass filtering and time-tapering are done to combat the unwanted effects of nonstationarity and/or spectral leakage

(e.g., Kaimal et al., 1989). A variety of techniques may be used including block averages, running mean filters, and no filtering at all (but rejecting samples where the cospectra are not well behaved at low frequency).

Application of the eddy correlation method requires measurements with sufficient frequency response to resolve the highest relevant components of the cospectrum – approximately $10U/z_r$. Even if a fast response sensor is available, it may not have sufficient resolution to provide meaningful signals for the chemical species of interest (Businger and Delaney, 1990). If a slow response sensor is available which can resolve very small concentration differences, then the Relaxed Eddy Accumulation (REA) method can be employed (Businger and Oncley, 1990). REA is a conditional sampling method where air is pumped into reservoirs depending on the vertical velocity. In the original eddy accumulation method (Hicks and McMillen, 1984), the pumping speed was varied proportionally to the vertical velocity. In the *relaxed* eddy accumulation method, the reservoirs are selected based on a vertical velocity threshold, w_0, but the filling rate is constant. The flux is computed from the difference in concentration difference between 'up' and 'down' reservoirs,

$$F_s = b_\chi \sigma_w (\mathrm{X}_{up} - \mathrm{X}_{dn}), \tag{55}$$

where σ_w is the standard deviation of vertical velocity and the coefficient b_χ depends on the threshold and z/L (Andreas et al., 1998; Businger and Oncley, 1990; Oncley et al., 1993)

$$b_\chi = b_0(\zeta) \exp\left(-\frac{3}{4}\frac{w_0}{\sigma_w}\right). \tag{56}$$

For joint-Gaussian turbulence (a good approximation to scalars in neutral conditions), $b_0(0) = 0.63$ for a threshold of zero. If sensor noise and any mean bias in the concentration difference measurement are negligible, then the optimal velocity threshold is about σ_w (Oncley et al., 1993).

7.2. MOST METHODS

The primary MOST-based flux estimation methods in use are the gradient/profile, the bulk, the variance, and the inertial-dissipation methods. As stated before, these methods rely on dimensionless functions that must be determined empirically using covariance measurements as the standard. Most of the relevant functions have been first measured overland and then either assumed or verified to be applicable over the ocean. Bulk methods were discussed in Section 2 and, except for obtaining friction velocity or stability, are irrelevant to the determination of V_t (i.e., you need V_t to use the bulk method). We will not discuss every method in detail here but will briefly describe the inertial-dissipation method as an example and then comment on strengths and weaknesses of some of the other methods. The variance method is described by Kaimal and Finnigan (1994) and Jodwalis and Benner (1996); the

gradient (profile) method is described by Kraus and Businger (1994) and Lenschow (1995).

The inertial-dissipation flux method is based on MOST forms for the high-frequency portion of the variance spectrum, Φ_χ, which goes as $\omega^{-5/3}$, where ω is the angular frequency. This portion of the spectrum is characterized by the structure-function parameter, C_χ^2, for the variable χ by (Wyngaard et al., 1971),

$$C_\chi^2 = 4U^{-2/3}\omega^{5/3}\Phi_\chi(\omega). \tag{57}$$

The structure function is then related through MOST,

$$C_\chi^2 = \chi_*^2 z^{-2/3} f_\chi(\zeta), \tag{58}$$

where a form is specified (Edson and Fairall, 1998) for the dimensionless function $f_\chi(\zeta)$ and measured values for C_χ^2 are used to solve for χ_*. This method has been used extensively to measure drag coefficients over the open ocean (Yelland et al., 1994); see reviews by Fairall and Larsen (1986) and by Edson et al. (1991). A variation on this approach is to convert the structure functions to dissipation rates and then use MOST dissipation forms such as (49).

The main attraction of the inertial-dissipation method is its use of the high-frequency portion of the spectrum where platform motions are overwhelmed by the turbulence signal; thus, ship motion corrections and precise vertical alignments are not required (because streamwise and cross-stream velocity spectra are different in the inertial subrange, some attention must be paid to orientation/alignment). However, the inertial subrange occurs at frequencies higher than the upper frequency limit of the covariance method (Section 7.2), so this method requires even faster response sensors. Internal sensor white noise is not coherent with vertical velocity, so its contribution to the w–χ cospectrum is rapidly reduced by averaging in the eddy correlation flux measurement. This is not true for the variance spectrum used in the inertial-dissipation method, so the requirements for low sensor noise are more critical. Some work has been done in applying this method to gas fluxes over the ocean for sulfur gases (Jodwalis and Benner, 1996) and to CO_2 (Larsen et al., 1997). With continued improvements in ship motion measurements, it is likely that use of the inertial-dissipation method for trace gas fluxes will diminish.

The gradient method has been used extensively overland for the measurement of trace gas fluxes (Baldocchi et al., 1988; Simpson et al., 1997), but its application over the ocean is rare. The fluxes tend to be small, so the concentration difference between two levels is very small. This places demands on measurement resolution similar to the REA method. The gradient method has a major advantage over REA in that high-speed, near-instantaneous, motion-corrected measurements of vertical velocity are not required, so it is attractive for application on ships. This advantage is partly compensated by a much greater sensitivity to surface-layer stability (i.e., the stability functions in (5) and (6) are much more variable than b_0); however, the REA method is relatively new and the characteristics of the coefficients have

not been extensively studied. Also from (5) we can see that the gradient goes approximately as $1/z$, so accuracy is improved by making one measurement near the surface. Note that over a fixed surface, (5) is valid for $z > 100z_0$, which is about 1–10 mm over the ocean (see Figure 3). The ocean is one of the least rough aerodynamic surfaces studied by micrometeorologists, but it is, paradoxically, difficult to make measurements near the surface because of metre-scale surface waves. All flux measurement methods from ships are compromised by flow distortion, but the gradient method is most sensitive. Also, measurements from ships are even more difficult because of exaggerated motion near the bow where most sensors or intakes are placed. Air sampling is usually done through long tubes with different intake heights that are plumbed to a single sensor; measurements are multiplexed, or in some cases, the difference is measured directly to avoid errors caused by possible mean offsets of two different sensors. However, sea spray concentrations increase near the surface, so it is difficult to prevent differential contamination of the sample tubes and/or their inlets. Interactions of trace gases and oceanic contaminants can lead to tube-induced biases that cause errors in flux estimates.

7.3. Air density fluctuations (the Webb et al. correction)

In Section 2, we wrote the conservation equation for mass concentration, X, and used the turbulent flux in the form $\overline{w'\chi'}$. This is an approximation to the fundamentally conservative expression of the flux (Businger, 1982),

$$F_\chi = \rho_a \overline{w' r'_\chi}, \tag{59}$$

where r_χ is the mixing ratio for χ, defined as the mass of χ per unit mass of dry air

$$r_\chi = \frac{m_\chi p_\chi}{m_a (p - p_v - p_\chi)}, \tag{60}$$

where m is the molecular weight, p the total atmospheric pressure, p_v the partial pressure for water vapour, and p_χ for the trace constituent with density, χ,

$$\chi = p_\chi m_\chi / (R_{\text{gas}} T). \tag{61}$$

If the scalar sensor measures the mixing ratio, then its correlation with vertical velocity can be used with (59) to compute the flux. If the scalar sensor measures mass concentration, then the flux must be corrected (Bakan, 1978; Webb et al., 1980). If we require that p and r_χ are unchanged by fluctuations in water vapour concentration, ρ'_v, and temperature, T', then

$$\rho_a r'_\chi = \chi' + \left[\frac{m_a \rho'_v}{m_v \rho_a} + \left(1 + \frac{m_a \rho_v}{m_v \rho_a} \right) \frac{T'}{T} \right] \mathrm{X}. \tag{62}$$

Note that in the absence of fluctuations of mixing ratio, fluctuations of temperature and/or humidity will cause fluctuations in χ. This is sometimes referred to as the *dilution effect* because an increase in moisture or temperature will cause a decrease in χ.

If mass concentration is measured, the dilution effect is relevant to all forms of micrometeorological flux estimation (eddy-correlation, variance, inertial-dissipation, or gradient) and (62) is used to determine the corrections. For example, the effect on the eddy-correlation flux is found by multiplying by w' and taking the average

$$\begin{aligned} V_t \Delta \mathrm{X} &= \overline{w'\chi'} + \left[\frac{m_a}{m_v \rho_a} \overline{w'\rho_v'} + \left(1 + \frac{m_a \rho_v}{m_v \rho_a} \right) \frac{\overline{w'T'}}{T} \right] \mathrm{X} \\ &= \overline{w'\chi'} + \bar{w}\mathrm{X}, \end{aligned} \tag{63}$$

where $\bar{w}$ is a very small mean vertical velocity required to maintain constant density of dry air in the presence of sensible and latent heat transfers. Thus, eddy-correlations computed from mass-concentration sensors can be corrected with specification of the sensible and latent heats and the mean concentration, X. The effect on the gradient method can be assessed by converting (62) to a vertical derivative; the effect on variance and inertial dissipation methods by squaring (62) and averaging to convert to variances (with a $\rho_v' T'$ cross term). If coincident high-speed time series of ρ_v' and T' are available, then (62) can be applied to the time series of χ', in which case no further corrections are necessary. This approach has the advantage that variance spectra and w–χ cospectra can be computed without interference from temperature and moisture.

For scalar sensors with closed paths, there is the possibility to eliminate the dilution effect by drying and thermalizing the air before detection of χ, which is equivalent to measuring r_χ. This approach is particularly attractive (Lee et al., 1994; Leuning and Judd, 1996; Leuning and Moncrieff, 1990) for trace gas work where $\bar{w}$ can be comparable to V_t and ΔX is usually small compared to X. Examples of $\bar{w}$ as functions of wind speed are shown in Figure 5 for some typical marine boundary layer conditions (sea-air temperature difference of 1.5C and RH of 82%) in comparison to estimates of CO_2 transfer velocity (see Section 6.3). For the situations shown in Figure 5, $\bar{w}$ is about twice the transfer velocity, which means that the dilution effect must be determined very accurately, or the field programs must be conducted in regions where ΔX/X is large. This issue is discussed more quantitatively in Section 7.5.

7.4. SENSOR CROSS-SENSITIVITIES

Interference of one chemical species with another has long been a problem in trace gas analysis. Optical absorption techniques are common in fast response and highly accurate mean sensors used in this work. In the case of CO_2, there are several optical absorption sensors available: the closed-path LI-COR LI-6262 model

series; the Oak Ridge sensor (Auble and Meyers, 1992); the KNMI Infrared Flux Meter (Kohsiek, 1991); and the Advanet sensor (Ohtaki and Matsui, 1982). These instruments typically use narrow filters to isolate portions of the spectrum with strong CO_2 absorption, strong water vapour absorption, and a reference with little or no absorption by either species. The filters are imbedded in a rotating disc and light from a single source is detected after passing through each of the filters. Both CO_2 and water vapour concentrations are computed from the three signal values. Kohsiek (1998b) identified five sources of H_2O/CO_2 cross-sensitivity: absorption by water vapour in the selected CO_2 filter band, absorption by water vapour in the spectral region not completely rejected by the CO_2 filter band, water dimers (loosely bonded pairs of water vapour molecules), pressure broadening, and the presence of liquid water on the optics in the form of droplets or a thin film. The cross-sensitivity is usually expressed as the dimensionless coefficient, β, which is the apparent CO_2 mass concentration fluctuation caused by a given water vapour mass concentration fluctuation. For example, the LI-COR manual gives a value $\beta = 1.4 \times 10^{-4}$ for the LI-6262. The dilution effect is a form of cross-sensitivity; we can take the water vapour component from (62) and write an equivalent dilution cross-sensitivity coefficient,

$$\beta_d = -\frac{m_\chi}{m_v}\frac{p_\chi}{p}. \tag{64}$$

For CO_2, e/p is about 3.6×10^{-4}, so $\beta_d \approx -9 \times 10^{-4}$. The dilution effect also causes a temperature cross-sensitivity, but there may be optical sources of other forms of temperature cross-sensitivity (Mestayer and Rebattet, 1985).

Calibration chambers can be used to estimate β in carefully controlled conditions. Leuning and King (1992) found $\beta = 2.5 \times 10^{-4}$ for a LI-COR model LI-6251; Leuning and Judd (1996) found a value of $\beta = 3 \times 10^{-3}$ for an Advanet model E009 and near-zero value for an Oak Ridge sensor. For the KNMI/IFM sensor, Kohsiek (1998b) found values for β varying between 4.2 and -2.9×10^{-4}, depending on the choice of absorption filter bandwidth and reference filter wavelength. Presumably, negative cross-sensitivities are the result of a greater water vapour effect in the reference band than the CO_2 absorption band. Under dry (low relative humidity) conditions, Kohsiek (1998b) found a near-zero (2.5×10^{-5}) coefficient for the Oak Ridge, in agreement with Leuning and Judd (1996). However, under humid conditions, the Oak Ridge sensor showed a large sensitivity that was a strong function of relative humidity. This behaviour was not observed with the KNMI/IFM sensor. While both sensors have heated windows, the Oak Ridge has unheated mirrors as part of the optical path, so it is hypothesized that this increased cross-sensitivity is associated with water vapour interactions with the optical surfaces.

A different type of cross-sensitivity has been discovered on recent ship-based measurement programs (Smith, private communication). The optical sensors use rotating filter or chopper wheels and their speeds are apparently affected by ship

motions. There is also some possibility that optical paths are distorted by wave-induced accelerations. Either or both of these effects apparently cause some cross-sensitivity of both CO_2 and water vapour concentrations with ship motion. Because motion corrections for vertical velocity are not perfect, there is some possibility of artificial correlations with motion-corrected vertical velocity fluctuations and measured CO_2 concentrations.

For example, let us define a new cross-sensitivity coefficient, μ, which characterizes the apparent fluctuation in CO_2 caused by an acceleration of the sensor in the spirit of β

$$\chi' = \mu X_{ar} a'. \tag{65}$$

We now express the actual computed motion-corrected vertical velocity, w_c', as the true vertical velocity plus some residual *error* in the motion corrections

$$w_c' = w' + \delta w_m. \tag{66}$$

This will cause the computed eddy correlation to be in error

$$\begin{aligned} \overline{w'\chi'} &= \overline{w_c'\chi'} - \mu \mathrm{X}_{ar} \eta \overline{w_m(\boldsymbol{\xi}, t) a_m(\boldsymbol{\xi} + \mathrm{d}\boldsymbol{\xi}, t + \mathrm{d}t)} \\ &= \overline{w_c'\chi'} - \mu \mathrm{X}_{ar} \eta \sigma_{wm} \sigma_{am} r_{wa}(\mathrm{d}\boldsymbol{\xi}, \mathrm{d}t), \end{aligned} \tag{67}$$

where we have $\delta w_m' = \eta w_m$ as a fraction of the motion correction applied to the raw velocity, and we have represented the cross-correlation in terms of the standard deviations of vertical motion and acceleration and the dimensionless cross-correlation coefficient, r_{wa}, of the motions. Here, we have made a distinction between the vertical velocity measured at time t and position $\boldsymbol{\xi}$ versus the concentration measurement made at position displaced from the anemometer by vector $\mathrm{d}\boldsymbol{\xi}$ with some time delay, $\mathrm{d}t$. This accounts for cases where the gas sensor is physically displaced from the anemometer and for time delays associated with long air sample tubes.

For collocated w and χ measurements, the correlations of vertical components in (67) will not contribute to the eddy gas flux (velocity and acceleration are in quadrature for periodic motion), but vertical velocity may correlate with horizontal accelerations. For displaced measurements, the correlation will approach zero as $\mathrm{d}t$ becomes large (several wave periods). In general, the behaviour of the correlation in (67) will be complicated, but should be amenable to empirical determination for a given experimental setup. The coefficient η is on the order of 0.1 and can be reduced by improved motion correction methods. The coefficient μ can be determined in simple laboratory studies and can also be reduced by improved instrument design. On a recent cruise in the N. Atlantic aboard the R/V Knorr, a simple fit to the motion corrections at the sensor mast gave

$$\begin{aligned} \sigma_{wm} &= 0.74 + 0.039 U_{10}, \\ \sigma_{um} &= 0.50 + 0.025 U_{10}. \end{aligned} \tag{68}$$

Note that for wave-induced motion, $\sigma_{am} = (2\pi/T_{\text{wave}})\sigma_{um} \approx \sigma_{um}$ sec^{-1} (for typical 6 sec waves). As an example, measurements made on the GASEX-98 cruise (see Section 8.3) indicated that a horizontal acceleration of 1 m s^{-2} produces a fluctuation from the LI-6262 sensor of 0.1 μatm when X_{ar} = 360 μatm; thus, $\mu = 2.8 \times 10^{-4}$. Therefore, at a wind speed of 10 m s^{-1}, the 'true' value for the flux will be about $10^{-4}\Delta X$ (i.e., V_t = 30 cm h^{-1}), while the second term in (67) will be about $2.0 \times 10^{-5} X_{ar} r_{wa}$. If r_{wa} is near one, then this level of sensor-motion cross-sensitivity will be significant.

7.5. Flux uncertainties

The uncertainty in micrometeorological determinations of gas transfer properties are primarly linked to uncertainties in the flux measurements. These include systematic biases and/or errors in sensor sensitivity, cross-sensitivities, experimental factors, and random noise and sampling uncertainties. Sensor errors are straightforward and require no further discussion; cross-sensitivities were discussed in Sections 7.3 and 7.4. Experimental factors include physical separation of sensors that are being cross-correlated (Kristensen et al., 1997; Lee and Black, 1994), loss of correlation by mixing in gas sample tubes (Leuning and Judd, 1996; Rannik et al., 1997), and other standard issues in micrometeorological methods (Businger, 1986; Horst and Weil, 1994). Non-random sources of error can only be reduced by better sensors, improved exposure, and improved measurement techniques. The contributions of random error can be reduced by averaging over larger and larger samples. Because gas transfer involves a number of physical parameters, development of a database with a sufficient ensemble of environmental conditions requires a number of field expeditions.

To discuss the random aspects of application of eddy correlation measurements to gas transfer, we start with an expression for the sampling uncertainty in the covariance flux,

$$\Delta F_\chi = \Delta(\overline{w'\chi'}) \approx \frac{\sigma_w \sigma_\chi}{(T/\tau_i)^{1/2}}, \tag{69}$$

where σ_χ is the standard deviation of fluctuations of concentration in χ from all sources including instrumental noise, T the length of the averaging period, and $\tau_i \approx 12z/U$, the integral time scale for vertical velocity fluctuations (Fairall, 1984). We will consider three components to the variance of χ: (1) surface flux induced, σ_{χ_t}, (2) atmospheric processes leading to χ fluctuations not associated with surface exchange (i.e., uncorrelated with w' near the surface), σ_{χ_r}, and (3) random internal sensor noise, σ_{χ_n}, at the integral time scale. The first is straightforwardly represented by MOST

$$\sigma_{\chi_t} \approx 3\chi_* = 3|F_s|/u_* = 3V_t|\Delta X|/u_*. \tag{70}$$

The second contribution is represented as a fraction, γ, of the background atmospheric concentration

$$\sigma_{\chi_r} = \gamma \mathrm{X}_{ar}. \tag{71}$$

The random noise is estimated assuming the sensor noise is characterized by a white noise variance spectrum, Φ_{χ_n}

$$\sigma^2_{\chi_n} = \Phi_{\chi_n}/\tau_i. \tag{72}$$

For the CO_2 instruments discussed in Section 8.3, Φ_{χ_n} is about 7×10^{-15} Hz^{-1} or 2.7×10^{-3} μatm^2 Hz^{-1}. Assuming that the total variance is the sum of the three components, we can show that

$$\Delta(F_s)/F_s = \frac{3\sigma_w/u_*}{(U\mathrm{T}/12z_r)^{1/2}} \left[1 + \left(\frac{\gamma \mathrm{X}_{ar}}{2\Delta \mathrm{X} V_t/u_*}\right)^2 + \left(\frac{\sigma_{\chi_n}}{2\Delta \mathrm{X} V_t/u_*}\right)^2\right]^{1/2}. \tag{73}$$

In near neutral conditions, σ_w/u_* will be about 1.2; for wind speeds less than 10 m s^{-1} (i.e., in the absence of significant bubble effects), the quantity V_t/u_* will be relatively independent of wind speed. This equation illustrates the limitations of the eddy correlation method and tells us the experimental factors that promote accurate determinations of the flux: larger averaging times, wind speed, sea-air concentration difference, and transfer velocity; measurements closer to the surface; small sensor internal noise; and an absence of other sources (e.g., entrainment, horizontal inhomogeneity, or pollution plumes) of concentration variance. If the last two terms in (73) are negligible, then z_r = 20 m, U = 10 m s^{-1}, and T = 30 min yields a random flux uncertainty of 0.45. Some of these aspects are subject to instrumentation design (σ_{χ_n}), and experiment design (z_r and possibly ΔX or γ), while others depend on nature.

Error analysis of the REA method is similar to (73) except the value for the threshold (Oncley et al., 1993) and any mean bias in concentration difference must be considered. Error analyses of the bulk (Blanc, 1985), gradient (Blanc, 1983), and inertial-dissipation (Edson et al., 1991) methods are available in the literature. With the MOST methods, sampling errors are reduced compared to the eddy-correlation method because first and second moments converge more quickly than cross-covariances. However, MOST methods have additional errors caused by uncertainty in the stability functions and by feedback effects associated with iterations to determine ζ (error due to the feedback effect may be reduced by using bulk estimates of ζ).

8. Recent Micrometeorological Field Programs

8.1. BACKGROUND

Early efforts in direct micrometeorological measurements of CO_2 gas flux over the ocean (Smith et al., 1991; Smith and Jones, 1985; Wesely et al., 1982) yielded unexpected results and triggered the controversy discussed in Section 1. These early studies were performed from towers on the beach or near the surf zone, which may have had some effect on their results. Recently, several studies have been done from offshore platforms and ships with improved sensors and renewed attention to experimental problems uncovered in the earlier work. Transfer velocity results from these studies are shown in Figure 6. These include ship-based (motion-corrected) eddy-correlation measurements on Lake Ontario (Donelan and Drennan, 1995) using a sonic anemometer and a LI-COR model LI-6262 with a 2-m sample tube. A second brief study was conducted by McGillis and Edson (1997) off the Massachusetts coast using a similar setup; ΔpCO_2 was 80–150 μatm, so CO_2 measurements were made with good signal-to-noise. We have also included estimates of CO_2 transfer velocity (Hausecker and Jahne, 1995) made by analogy with the oceanic molecular sublayer temperature gradient (cool skin) ΔT_{cool}

$$k_\chi = \frac{R_{nl} + H_s + H_l}{\rho_w c_{pw}} \Delta T_{\text{cool}}^{-1} (P_r / S_c)^{1/2}, \tag{74}$$

where R_{nl} is the net longwave radiative flux at the sea surface, H_s is the sensible heat flux, H_l is the latent heat flux, and P_r is the Prandtl number in water.

8.2. ASGAMAGE

In the fall of 1996, the third in a series of Air–Sea Gas Transfer and Marine Aerosol Generation (ASGAMAGE) studies (Oost, 1995; Oost, 1998) was conducted on the Dutch North Sea offshore facility *Meetpost Noordwijck* and was hosted by the Royal Dutch Meteorological Institute (KNMI). Fifteen European and North American research groups participated in a comprehensive study of various aspects of air–sea interaction with an emphasis on micrometeorological measurements of trace gas fluxes. Conditions were favourable for large CO_2 signals with ΔpCO_2 between 50 and 160 μatm. Some exploratory work was done with REA and gradient measurements (Dissly et al., 1998), but we will limit our discussion here to eddy-correlation measurements of CO_2 flux made using a sonic anemometer with two different open-path fast CO_2 sensors – the Oak Ridge (Auble and Meyers, 1992) and the KNMI/IFM (Kohsiek, 1991) sensors. Cross-sensitivity studies (Section 7.4) indicate that the KNMI/IFM sensor, by virtue of its heated optics, has well-characterized water vapour cross-sensitivity, while the Oak Ridge sensor, which has unheated mirrors, is subject to greater and more variable cross-sensitivity. The Oak Ridge mirror and optics were washed off frequently, but this

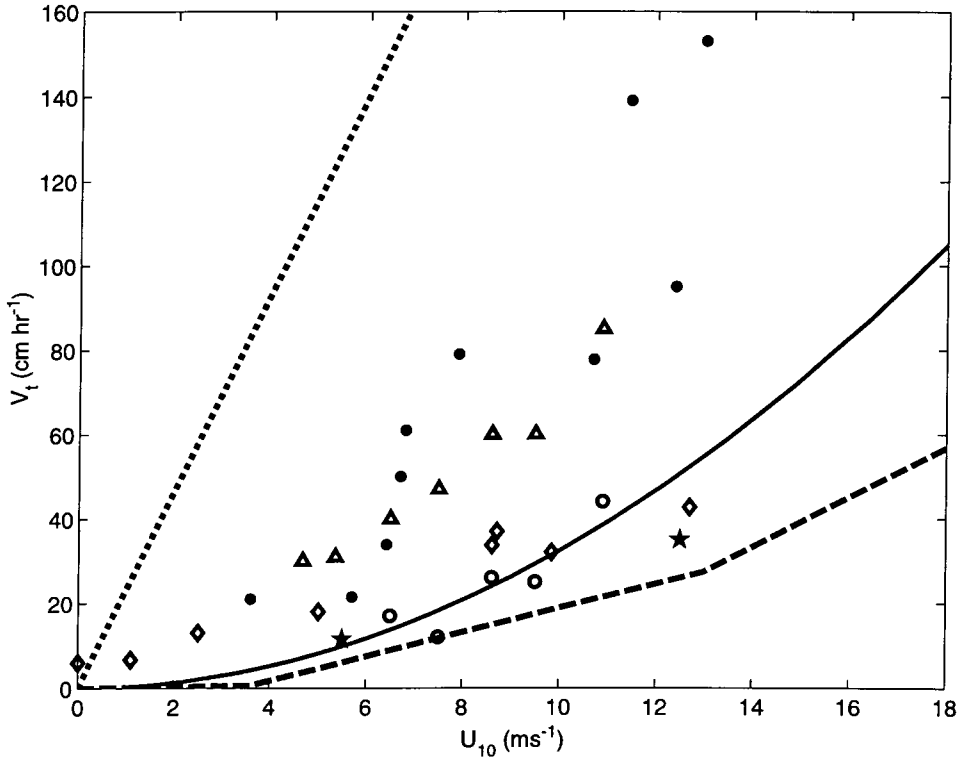

Figure 6. CO_2 transfer velocity at $S_c = 600$ versus 10-m wind speed. The lines are as in Figure 1. The points are from recent field programs: solid circles (Donelan and Drennan, 1995); stars (McGillis and Edson, 1997); diamonds (Hausecker and Jahne, 1995); open circles, ASGAMAGE KNMI/IFM sensor; triangles, ASGAMAGE Oak Ridge sensor. The triangles and open circles are for water temperatures around 8–12 °C; the others are for temperatures around 15–20 °C.

measure may have been insufficient to maintain cleanliness. The platform is stable, so motion corrections and cross-sensitivities are not applicable; flow distortion and other cross sensitivities, of course, remain.

The time series of $\overline{w'\chi'}$ and $\bar{w}\mathrm{X}$ were highly anti-correlated, which follows from (63); if the net flux is a small residual of two terms that roughly cancel (i.e., if $V_t \Delta \mathrm{X} \approx 0$), then we expect $\overline{w'\chi'} \approx -\bar{w}\mathrm{X}$. The total means from 91 1-h CO_2 flux values ($\overline{w'\chi'}$) were -0.011 mg m^{-2} s^{-1} for the Oak Ridge sensor, -0.037 mg m^{-2} s^{-1} for the KNMI/IFM sensor, and +0.045 mg m^{-2} s^{-1} for the dilution (Webb) effect at a mean wind speed of 9 m s^{-1} and ΔpCO_2 of 66 μatm. The resolution for a 1-h flux measurement is about 0.02 mg m^{-2} s^{-1} for the Oak Ridge sensor (Auble and Meyers, 1992), so the random uncertainty in the mean of 90 points is about 0.002 mg m^{-2} s^{-1}. For the KNMI/IFM sensor, the dilution-corrected flux was about 20% of each of the two measured quantities. Fluxes from these instruments have been converted to transfer velocity and averaged in wind speed bins (Fairall et al., 1997; Kohsiek, 1998a); the results are also shown in

Figure 6. The KNMI/IFM sensor values are fairly close to the Wanninkhof (1992) parameterization, while the Oak Ridge values are 2–3 times greater. These field and laboratory results led to the installation of heaters on the Oak Ridge mirrors. The disagreement between two well-calibrated sensors demonstrates the importance of cross-sensitivity for measurements of very small trace gas fluxes.

8.3. GASEX-98

In May–June of 1998, NOAA conducted a major oceanographic and meteorological study in a large CO_2 sink region in the N. Atlantic (46 N, 21 W) aboard the *R/V Ronald Brown* (see http://www.aoml.noaa.gov/general/project/ocdrhw5.html and http://www.aoml.noaa.gov/ocd/oaces/co2/natl98.html). Most of the study was made in a warm-core eddy with ΔpCO_2 between -80 and -100 μatm. Ranges for other variables were $1 <$ wind speed < 16 m s^{-1}; $55 <$ relative humidity $< 100\%$; $-85 <$ latent heat flux < 125 W m^{-2}; $-45 <$ sensible heat flux < 20 W m^{-2}; and $-1.6 < 10/L < 0.2$. GASEX-98 included measurements of a number of trace species in the ocean and atmosphere and determinations of gas transfer by dual-tracer, gradient, REA, budget, inertial-dissipation, and eddy-correlation methods. Atmospheric gas fluxes were measured for CO_2 and DMS.

We will discuss flux measurements using an open-path Oak Ridge sensor mounted on the ship's jackstaff and a closed-path LI-6262 located on a scaffold about 5 m back. The Oak Ridge was about 1 m from a sonic anemometer at a height of 19.5 m; the LI-6262 sampled through a tube with an inlet collocated with the sonic anemometer. A second LI-6262 was located in a laboratory about 40 m aft and sampled through a second tube with an inlet at the same sonic anemometer. The samples for the closed-path instruments were not dried; calculations indicated that the thermal fluctuations at the analyzers were negligible. The Oak Ridge had heated mirrors and the exposed optical surfaces were frequently washed with a system of fresh water hoses and spraying heads. Further details on sensors, motion corrections, and data processing are given in McGillis et al. (1999).

Processing and analysis of this large data set is in progress, but some preliminary results can be presented here. Sample variance spectra for moisture and CO_2 concentration are given in Figure 7 from the Oak Ridge and short-tube LICOR sensors. The moisture spectrum (Figure 7a) shows loss of high frequency signal in the LI-6262 associated with smoothing effects in the sample tube. The results for CO_2 are similar, but the attenuation begins at a higher frequency. The greater damping of small-scale moisture fluctuations in sample tubes is often observed and is hypothesized to be caused by stronger surface interactions. The LI-6262 CO_2 concentration time series was corrected for the moisture-dilution effect and the moisture-broadening effect as per the LI-COR manual and then cross-correlated with the motion-corrected vertical velocity (with appropriate time lag). Raw flux values were rejected if the standard deviation of transverse motion corrections normalized by mean wind speed exceeded a threshold. This editing avoided situations

where motion-correction methods are known to have problems. Sample time series of CO_2 fluxes, ΔpCO_2, and wind speed are shown in Figure 8.

The fluxes were then converted to neutral stability and transfer velocities were computed. Transfer velocities computed with eddy-correlation fluxes from the LI-6262 are shown in Figure 9 after averaging in wind speed bins; 670 30-min values were used. Cospectra of w' and corrected fluctuations of CO_2 concentration were also averaged in wind-speed bins and examined (not shown). Some small influence is observed at a frequency corresponding to the peak in the surface wave spectrum, indicating either a true wave coupling to the scalar flux or some cross-sensitivity with ship motion. The average effect is less than 10%, although it tends to be larger at low wind speeds. Uncertainty in individual 30-min samples can be estimated from the standard deviation of transfer velocity values within each wind speed bin (Figure 10). The normalized uncertainty is about twice the random sampling error estimated in Section 7.5. Presumably, the other two random components and inadequate motion corrections contribute the remainder of the uncertainty. The decrease with increasing wind speed (a factor of 2.8 between 5 and 14 m s^{-1}) is somewhat stronger [a factor of $(14/5)^2 = 1.7$] than that expected from (63).

While the results presented here are preliminary and considerable laboratory work remains on cross-sensitivity issues, the consistency of these eddy-correlation values and the consensus curve from tracer experiments is certainly encouraging.

9. Conclusions

Bulk parameterization of water-air gas fluxes has been examined using turbulence scaling theory applied to both fluids. We have shown how one-fluid/two-layer and two-fluid/four-layer models can be related with simple representations of turbulent and molecular diffusive properties based on suppression of turbulent mixing near the boundary because of dissipation of small-scale eddies by viscosity. Analytical solutions can be obtained that reproduce the standard Schmidt number power laws ($-1/2$ for surface renewal and $-2/3$ for conventional smooth flow) for the scalar molecular sublayer resistance. Buoyancy effects, which lead to significant gas transfer at zero vector mean wind speed for convective conditions, are naturally incorporated through the MOST stability length and the molecular sublayer Richardson number.

Unfortunately, our mathematically elegant model does not capture all of the relevant physics of the transfer processes. We have presented some recent treatments of wave turbulence and bubble-mediated enhancements. They can be adjusted to give ‘reasonable looking’ curves, but their physical generality is unknown. This is an active area of research with a bewildering variety of parameterizations on the market. We discussed possible effects of surfactants and sea spray, but offered no quantitative treatments. Some progress on the sea-spray and bubble problems might be made with numerical models. Major improvements in almost every

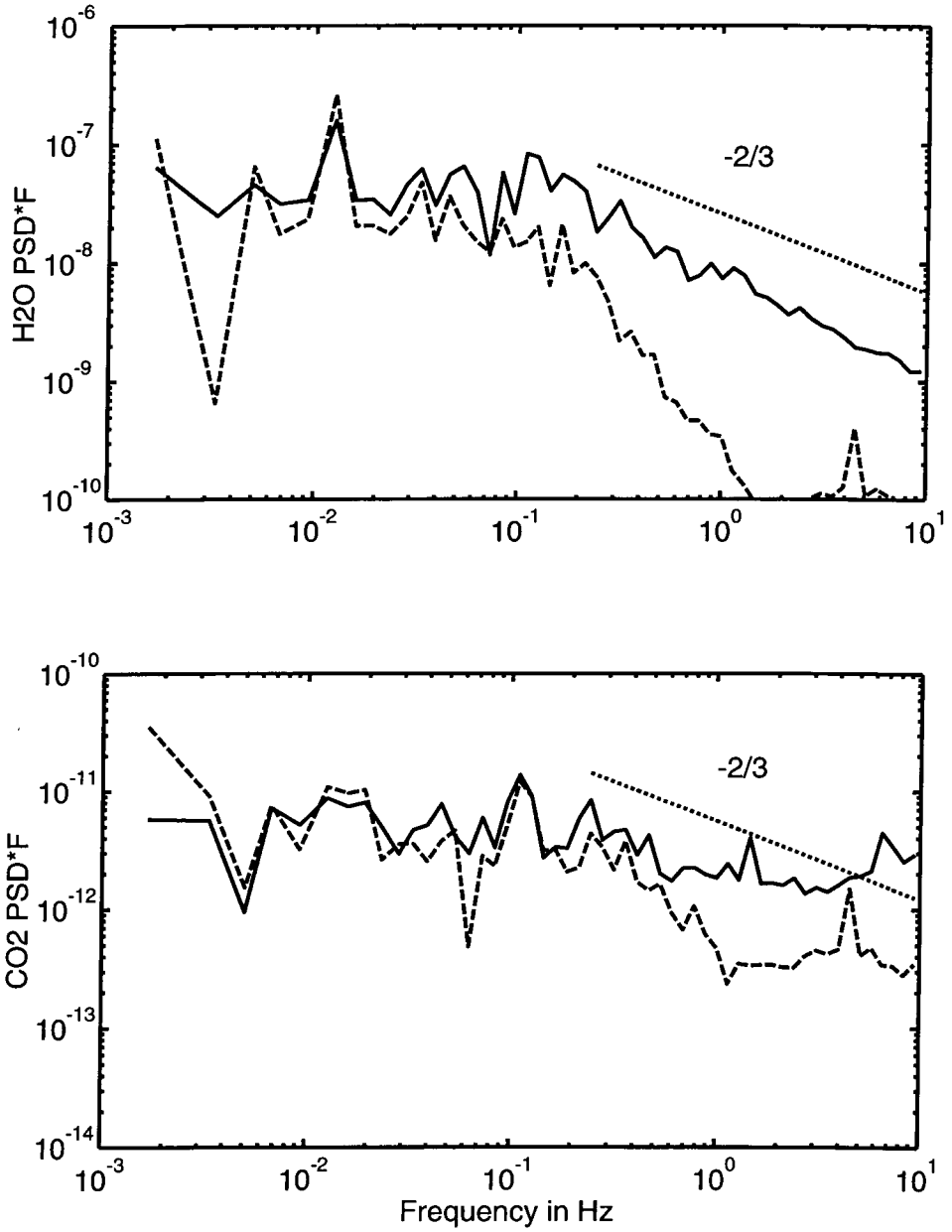

Figure 7. Sample variance spectra (multiplied by frequency) from the WHOI LI-6262 closed-path sensor (dashed line) and the ETL Oak Ridge open-path sensor (solid line) from GASEX-98: upper panel, moisture; lower panel, CO_2 concentration.

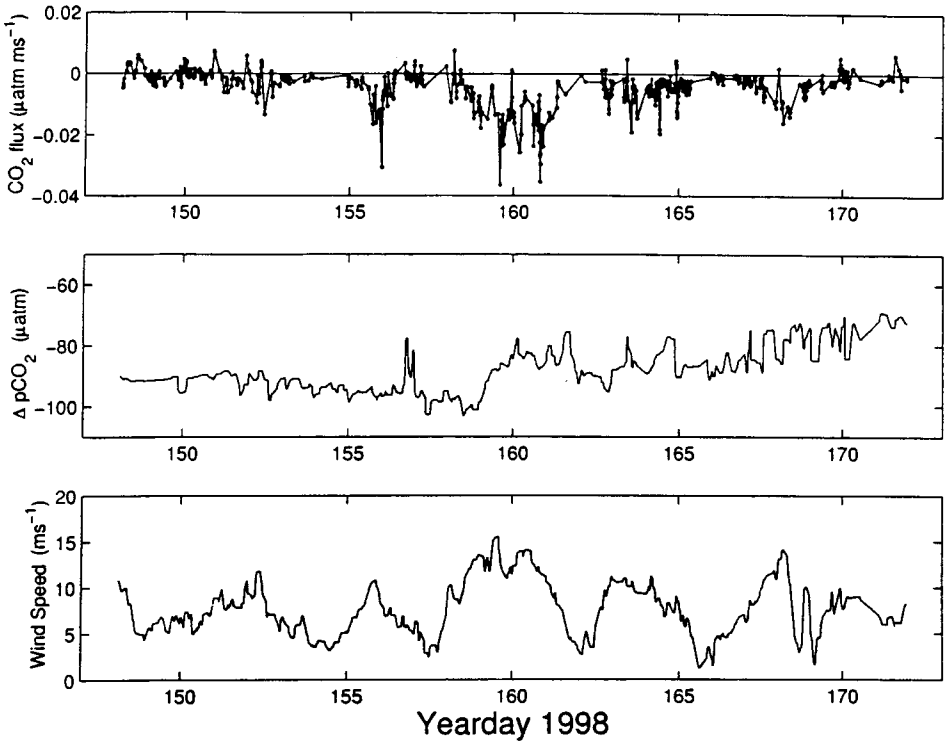

Figure 8. Time series of meteorological properties from a section of the GASEX-98 cruise: upper panel, CO_2 flux; middle panel, mean sea-air CO_2 pressure difference; and lower panel, wind speed.

experimental aspect of these problems are required to completely resolve these issues.

In light of the controversy surrounding the micrometeorological versus laboratory and tracer methods of estimating gas fluxes, we discussed a host of issues involved in making high quality flux measurements from the atmospheric side. Some of these issues (sampling uncertainty, the dilution effect, fetch considerations, flow distortion) have been known (but perhaps their magnitude was unappreciated for the gas flux problem) since the 1970s but others (cross-sensitivities to water vapour, contamination of optics, and ship-motion) were virtually unknown. It is clear that the order-of-magnitude disagreements observed in the 1980s and early 1990s have been resolved in favor of the oceanographic community.

Ship-based and platform-based studies of the last few years have yielded eddy-correlation fluxes within a factor of three of a standard consensus parameterization (Wanninkhof, 1992). In one experiment (ASGAMAGE), two collocated and well-calibrated sensors yielded quite different values for CO_2 eddy-correlation fluxes which we take to be unambiguous proof of cross-sensitivity effects. The best and most recent study (GASEX-98) has yielded preliminary results very close to the nominal curve. It is also clear that improved fast CO_2 sensors (with heated optics

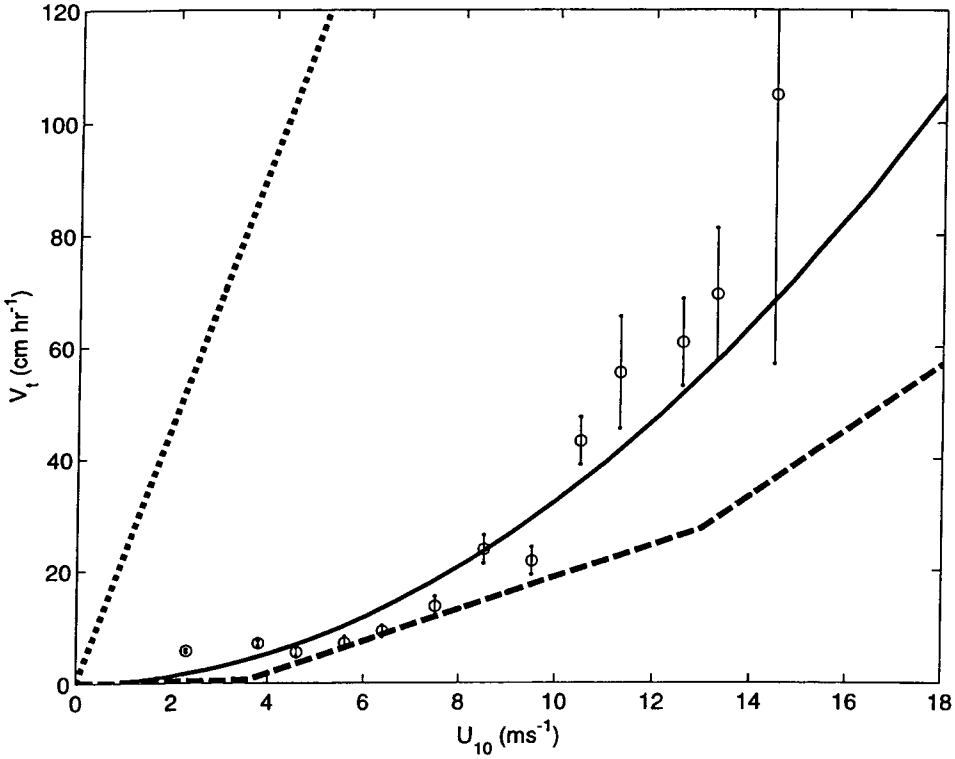

Figure 9. CO_2 transfer velocity at $S_c = 600$ versus 10-m wind speed. The lines are as in Figure 1. The points are wind-speed bin averages from the WHOI LI-6262 in the GASEX-98 field program. The error bars are the uncertainty of the mean estimate computed using the standard deviation of values and the number of samples within each bin.

if open path) are critical to these improved results. However, it would be a mistake to attach great significance to this result simply because it agrees with Wanninkhof (1992). The real significance must come from a careful examination of all of the pitfalls inherent in the eddy-correlation method, the sensors we are using, the quality of ship motion corrections, and consistency with other methods (tracer, gradient, REA) that were used on that experiment.

Acknowledgments

This work is supported at WHOI by the National Science Foundation Ocean Science and Technology program and at ETL by the NOAA Ocean-Atmosphere Exchange of Carbon Exchange Studies component of the Climate and Global Change Program. The authors wish to thank Wiebe Oost for aid rendered during hosting of the ASGAMAGE experiment and Rik Wanninkhof and Jim Butler for their fine stewardship of the GASEX-98 cruise. We also appreciate the help and

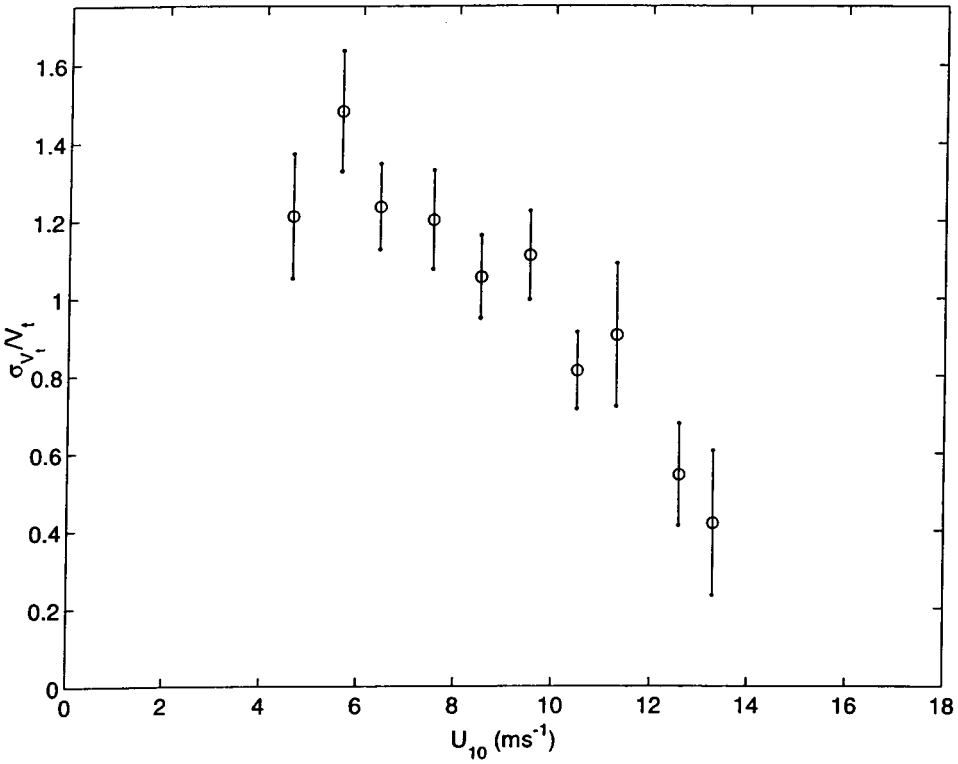

Figure 10. Normalized uncertainty in individual 30-min eddy-correlation transfer velocity estimates for data from Figure 9. Bins with fewer than five samples were not used in this plot.

cooperation of the captain and crew of the *R/V Ronald Brown*. This manuscript was improved by comments from two anonymous referees.

References

Andreas, E. L.: 1992, 'Sea Spray and the Turbulent Air–Sea Heat Fluxes', *J. Geophys. Res.* **97**, 11429–11441.

Andreas, E. L.: 1998, 'A New Sea Spray Generation Function for Wind Speeds Up to 32 m/s', *J. Phys. Oceanog.* **28**, 2175–2184.

Andreas, E. L. and DeCosmo, J.: 1999, 'Sea Spray Production and Influence on Air–Sea Heat and Moisture Fluxes over the Open Ocean', in G. L. Geernaert (ed.), *Air–Sea Fluxes of Momentum, Heat, and Chemicals*, Kluwer Academic Publishers, Dordrecht, to appear.

Andreas, E. L., Edson, J. B., Monahan, E. C., Rouault, M. P., and Smith, S. D.: 1995, 'The Spray Contribution to Net Evaporation from the Sea: A Review of Recent Progress', *Boundary-Layer Meteorol.* **72**, 3–52.

Andreas, E. L., Hill, R. J., Gosz, J. R., Moore, D. I., Otto, W. D., and Sarma, A. D.: 1998, 'Stability Dependence of the Eddy-Accumulation Coefficients for Momentum and Scalars', *Boundary-Layer Meteorol.* **86**, 409–420.

Asher, W. and Wanninkhof, R.: 1998a, 'The Effect of Bubble-Mediated Gas Transfer on Purposeful Dual-Tracer Experiments', *J. Geophys. Res.* **103**, 10555–10560.

Asher, W. and Wanninkhof, R.: 1998b, 'Transient Tracers and Air–Sea Gas Transfer', *J. Geophys. Res.* **103**, 15939–15958.

Asher, W. E., Karle, L. M., Higgins, B. J., Farley, P. J., Monahan, E. C., and Leifer, I. S.: 1996, 'The Influence of Bubble Plumes on Air–Seawater Gas Transfer Velocities', *J. Geophys. Res.* **101**, 12027–12041.

Auble, D. L. and Meyers, T. P.: 1992, 'An Open Path, Fast Response Infrared Absorption Gas Analyzer for H_2O and CO_2', *Boundary-Layer Meteorol.* **59**, 243–256.

Bakan, S.: 1978, 'Note on the Eddy Correlation Method for CO_2 Flux Measurements', *Boundary-Layer Meteorol.* **13**, 597–600.

Baldocchi, D. D., Hicks, B. B., and Meyers, T. P.: 1988, 'Measuring Biosphere-Atmosphere Exchanges of Biologically Related Gases with Micrometeorological Methods', *Ecology* **69**, 1331–1340.

Beljaars, A. C. M.: 1994, 'The Parameterization of Surface Fluxes in Large-Scale Models under Free Convection', *Quart. J. Roy. Meteorol. Soc.* **121**, 255–270.

Blanc, T. V.: 1983, 'An Error Analysis of Profile Flux, Stability, and Roughness Length Measurements Made in the Marine Atmospheric Surface Layer', *Boundary-Layer Meteorol.* **26**, 243–267.

Blanc, T. V.: 1985, 'Variation of Bulk-Derived Surface Flux, Stability, and Roughness Results Due To the Use of Different Transfer Coefficient Schemes', *J. Phys. Oceanog.* **15**, 650–669.

Broecker, W. S. and Peng, T.-H.: 1974, 'Gas Exchange Rates between Air and Sea', *Tellus* **24**, 21–35.

Broecker, W. S., Ledwell, J. R., Takahashi, T., Weiss, L. M. R., Memery, L., Peng, T.-H., Jahne, B., and Munnich, K. O.: 1986, 'Isotopic versus Micrometeorological Ocean CO_2 Fluxes: A Serious Conflict', *J. Geophys. Res.* **91**, 10517–10527.

Brutsaert, W.: 1982, *Evaporation into the Atmosphere*, D. Reidel, Dordrecht, 299 pp.

Businger, J. A.: 1982, 'Equations and Concepts', in G. T. M. Nieuwstadt and H. v. Dop (eds.), *Atmospheric Turbulence and Air Pollution Modelling*, D. Reidel, Dordrecht, pp. 1–33.

Businger, J. A.: 1986, 'Evaluation of the Accuracy with which Dry Deposition can be Measured with Current Micrometeorological Techniques', *J. Clim. Appl. Meteorol.* **25**, 1100–1123.

Businger, J. A. and Delaney, A. C.: 1990, 'Chemical Sensor Resolution Required for Measuring Surface Fluxes by Three Common Micrometeorological Techniques', *J. Atm. Chem.* **19**, 399–310.

Businger, J. A. and Oncley, S. P.: 1990, 'Flux Measurement with Conditional Sampling', *J. Atmos. Oceanic Tech.* **7**, 349–352.

Chamberlain, A. C.: 1968, 'Transportation of Gases to and from Surfaces with Bluff and Wave Like Roughness Elements', *Quart. J. Roy. Meteorol. Soc.* **94**, 318–332.

Clayson, C. A., Curry, J. A., and Fairall, C. W.: 1996, 'Evaluation of Turbulent Fluxes at the Ocean Surface Using Surface Renewal Theory', *J. Geophys. Res.* **101**, 28503–28513.

Coantic, M.: 1980, 'Mass Transfer Across the Ocean–Air Interface: Small Scale Hydrodynamic and Aerodynamic Mechanisms', *Phys. Chem. Hydrodyn.* **1**, 249–279.

Csanady, G. T.: 1990, 'The Role of Breaking Wavelets in Air–Sea Gas Transfer', *J. Geophys. Res.* **95**, 749–759.

Dissly, R., Smith, J., and Tans, P.: 1998, 'Final Report on the NOAA/CMDL Contribution to ASGAMAGE-B', in O. Oost (ed.), *Proceedings of the ASGAMAGE Workshop*, KNMI, De Bilt, the Netherlands, 22–25 September, 1997, pp. 51–72.

Donelan, M. A. and Drennan, W. M.: 1995, 'Direct Field Measurements of the Flux of Carbon Dioxide', in B. Jahne and E. C. Monahan (eds.), *Air–Water Gas Transfer*, AEON Verlag & Studio, Hanau, Germany, pp. 677–683.

Edson, J. B. and Fairall, C. W.: 1998, 'Similarity Relationships in the Marine Atmospheric Surface Layer for Terms in the TKE and Scalar Variance Budgets', *J. Atmos. Sci.* **55**, 2311–2328.

Edson, J. B., Fairall, C. W., Mestayer, P. G., and S. E. Larsen: 1991, 'A Study of the Inertial-Dissipation Method for Computing Air–Sea Fluxes', *J. Geophys. Res.* **96**, 10689–10711.

Edson, J. B., Wetzel, S., Friehe, C. A., Miller, S., and Hristov, T.: 1997, 'Energy Flux and Dissipation Profiles in the Marine Surface Layer', in *Proceedings of the 12th Symposium on Boundary Layers and Turbulence*, 28 July–1 August, American Meteorology Society, Vancouver, BC.

Esbensen, S. K. and Reynolds, R. W.: 1981, 'Estimating Monthly Averaged Air–Sea Transfers of Heat and Momentum Using the Bulk Aerodynamic Method', *J. Phys. Oceanog.* **11**, 457–465.

Fairall, C. W.: 1984, 'Interpretation of Eddy-Correlation Measurements of Particulate Deposition and Aerosol Flux', *Atmos. Environ.* **18**, 1329–1337.

Fairall, C. W. and Larsen, S. E.: 1986, 'Inertial-Dissipation Methods and Turbulent Fluxes at the Air–Ocean Interface', *Boundary-Layer Meteorol.* **34**, 287–301.

Fairall, C. W., Bradley, E. F., Rogers, D. P., Edson, J. B., and Young, G. S.: 1996a, 'Bulk Parameterization of Air–Sea Fluxes for TOGA COARE', *J. Geophys. Res.* **101**, 3747–3764.

Fairall, C. W., Bradley, E. F., Godfrey, J. S., Wick, G. A., Edson, J. B., and Young, G. S.: 1996b, 'Cool Skin and Warm Layer Effects on Sea Surface Temperature', *J. Geophys. Res.* **101**, 1295–1308.

Fairall, C. W., Hare, J. E., Smith, S. D., Anderson, R. A., and Kohsiek, W.: 1997, 'Preliminary Analysis of CO_2 Flux Data from ASGAMAGE-B', in *Proceedings of the 12th Symposium on Boundary Layers and Turbulence*, Amer. Meteorol. Soc., 28 July–1 August, Vancouver, Canada, pp. 413–414.

Frew, N. M.: 1997, 'The Role of Organic Films in Air–Sea Gas Exchange', in P. S. Liss and R. A. Duce (eds.), *The Sea Surface and Global Change*, Cambridge University Press, Cambridge, U.K., pp. 121–172.

Fujitani, T.: 1985, 'Method of Turbulent Flux Measurement on a Ship by Using a Stable Platform System', *J. Meteorol. Soc. Japan* **36**, 157–170.

Garratt, J. R.: 1992, *The Atmospheric Boundary Layer*, Cambridge University Press, Cambridge, U.K., 316 pp.

Geernaert, G. L.: 1990, 'Bulk Parameterizations for the Wind Stress and Heat Fluxes', in G. L. Geernaert and W. J. Plant (eds.), *Surface Waves and Fluxes*, Kluwer Academic Publishers, Dordrecht, pp. 91–172.

Godfrey, J. S. and Beljaars, A. C. M.: 1991, 'On the Turbulent Fluxes of Buoyancy, Heat, and Moisture at the Air–Sea Interface at Low Wind Speeds', *J. Geophys. Res.* **96**, 22043–22048.

Hanawa, K. and Toba, Y.: 1987, 'Critical Examination of Estimation Methods of Long-Term Mean Air–Sea Heat and Momentum Transfers', *Ocean Air Interactions* **1**, 79–93.

Hasse, L.: 1990, 'On the Mechanism of Gas Exchange at the Air–Sea Interface', *Tellus* **42B**, 250–253.

Hasse, L. and Liss, P. S.: 1980, 'Gas Exchange across the Air–Sea Interface', *Tellus* **32**, 470–481.

Hausecker, H. and Jahne, B.: 1995, 'In situ Measurements of the Air–Sea Gas Transfer Rate during the MBL/CoOP West Coast Experiment', in B. Jahne and E. C. Monahan (eds.), *Air–Water Gas Transfer*, AEON Verlag & Studio, Hanau, Germany, pp. 775–784.

Hicks, B. B. and McMillen, R. T.: 1984, 'A Simulation of the Eddy Accumulation Method for Measuring Pollutant Fluxes', *J. Clim. Appl. Meteorol.* **23**, 637–643.

Horst, T. W. and Weil, J. C.: 1994, 'How Far Is Far Enough?: The Fetch Requirements for Micrometeorological Measurement of Surface Fluxes', *J. Atmos. Oceanic Tech.* **11**, 1018–1025.

Hunter, K. A.: 1997, 'Chemistry of the Sea–Surface Microlayer', in P. S. Liss and R. A. Duce (eds.), *The Sea Surface and Global Change*, Cambridge University Press, Cambridge, U.K., pp. 287–320.

Jahne, B. and Hausecker, H.: 1998, 'Air–Water Gas Exchange', *Annu. Rev. Fluid Mech.* **30**, 443–468.

Jahne, B. and Monahan, E. C.: 1995, *Air–Water Gas Transfer*, International Symposium on Air–Water Gas Transfer, AEON, Hanau, Germany, 910 pp.

Jodwalis, C. M. and Benner, R. L.: 1996, 'Sulfur Gas Fluxes and Horizontal Inhomogeneities in the Marine Boundary Layer', *J. Geophys. Res.* **101**, 4393–4401.

Kaimal, J. C. and Finnigan, J. J.: 1994, *Atmospheric Boundary Layer Flows – Their Structure and Measurment*, Oxford University Press, New York, NY, 400 pp.

Kaimal, J. C., Clifford, S. F., and Lataitis, R. J.: 1989, 'Effect of Finite Sampling on Atmospheric Spectra', *Boundary-Layer Meteorol.* **47**, 337–347.

Keeling, R. F.: 1993, 'On the Role of Large Bubbles in Air–Sea Gas Exchange and Supersaturation in the Ocean', *J. Mar. Res.* **51**, 237–271.

Kepert, J. and Fairall, C. W.: 1999, 'Modeling the Interaction between the Atmospheric Boundary Layer and Evaporating Sea Spray Droplets', in G. L. Geernaert (ed.), *Air–Sea Fluxes of Momentum, Heat, and Chemicals*, Kluwer Academic Publishers, Dordrecht, in press.

Kohsiek, W.: 1991, 'Infrared H_2O/CO_2 Sensor with Fiber Optics', in *Proceedings of the Seventh Symposium on Meteorological Observations and Instrumentation*, Amer. Meteorol. Soc., 14–18 January, New Orleans, LA, pp. 352–355.

Kohsiek, W.: 1998a, 'Measurement of CO_2 Flux with IFM during ASGAMAGE', in W. Oost (ed.), *Proceedings of the ASGAMAGE Workshop*, 22–25 September, KNMI, De Bilt, the Netherlands, 1997, pp. 33–37.

Kohsiek, W.: 1998b, *Water Vapor Cross-Sensitivity of Open Path H_2O/CO_2 sensors*, Report 98-15, Royal Netherlands Meteorological Institute, De Bilt, the Netherlands, 20 pp.

Kraus, E. B. and Businger, J. A.: 1994, *Atmosphere-Ocean Interaction*, Oxford, New York, 352 pp.

Kristensen, L., Mann, J., Oncley, S. P., and Wyngaard, J. C.: 1997, 'How Close Is Close Enough when Measuring Scalar Fluxes with Displaced Sensors', *J. Atmos. Oceanic Tech.* **14**, 814–821.

Lamont, J. C. and Scott, D. S.: 1970, 'An Eddy Cell Model of Mass Transfer into the Surface of a Turbulent Liquid', *A.I.Ch.E. J.* **16**, 513–519.

Larsen, S. E., Hansen, F. A., Kjeld, J. F., Lund, S. W., Kunz, G., and deLeeuw, G.: 1997, 'Experimental and Modeling Study of Air–Sea Exchange of Carbon Dioxide', in W. A. Ooost (ed.), *Proceedings of the ASGAMAGE Workshop*, Royal Dutch Meteorological Institute, De Bilt, the Netherlands, pp. 116–123.

Lee, X. and Black, T. A.: 1994, 'Relating Eddy Correlation Sensible Heat Flux to Horizontal Sensor Separation in the Unstable Atmospheric Surface Layer', *J. Geophys. Res.* **99**, 18545–18553.

Lee, X., Black, T. A., and Novak, M. D.: 1994, 'Comparison of Flux Measurements with Open- and Closed-Path Gas Analyzers above an Agricultural Field and a Forest Floor', *Boundary-Layer Meteorol.* **67**, 195–202.

Lenschow, D. H.: 1995, 'Micrometeorological Techniques for Measuring Biosphere-Atmosphere Trace Gas Exchange', in P. Mataon and R. Harris (eds.), *Biogenic Trace Gases: Measuring Emissions from Soil and Water*, Blackwell Science, Cambridge, MA, pp. 126–163.

Leuning, R. and Judd, M. J.: 1996, 'The Relative Merits of Open- and Closed-Path Analysers for the Measurement of Eddy Fluxes', *Global Change Biol.* **2**, 241–253.

Leuning, R. and King, K. M.: 1992, 'Comparison of Eddy-Covariance Measurements of CO_2 Fluxes by Open- and Closed-Path CO_2 Analysers', *Boundary-Layer Meteorol.* **59**, 297–311.

Leuning, R. and Moncrieff, J.: 1990, 'Eddy-Covariance CO_2 Flux Measurements Using Open- and Closed-Path CO_2 Analysers: Corrections for Analyser Water Vapour Sensitivity and Damping of Fluctuations in Air Sampling Tubes', *Boundary-Layer Meteorol.* **53**, 63–76.

Liss, P. S.: 1973, 'Processes of Gas Exchange Across an Air–Water Interface', *Deep-Sea Res.* **20**, 221–228.

Liss, P. S. and Merlivat, L.: 1986, 'Air–Sea Gas Exchange Rates: Introduction and Synthesis', in P. Buat-Manard (ed.), *The Role of Air–Sea Exchange in Geochemical Cycles*, D. Reidel, Norwell, MA, pp. 113–127.

Liu, W. T., Katsaros, K. B., and Businger, J. A.: 1979, 'Bulk Parameterization of the Air–Sea Exchange of Heat and Water Vapor Including the Molecular Constraints at the Interface', *J. Atmos. Sci.* **36**, 1722–1735.

Mahrt, L., Vickers, D., Howell, J., Hojstrup, J., Courtney, M., Wilczak, J. M., Edson, J. B., and Hare, J.: 1996, 'Surface Drag Coefficients in RASEX', *Boundary-Layer Meteorol.* **73**, 159–182.

Mangarella, P. A., Chambers, A. J., Street, R. L., and Hsu, E. Y.: 1973, 'Laboratory Studies of Evaporation and Energy Transfer through a Wavy Air–Water Interface', *J. Phys. Oceanog.* **3**, 93–101.

McGillis, W. R. and Edson, J. B.: 1997, *An Investigation of Gas Transfer Coefficients Using Direct Estimates of the CO_2 Flux*, WHOI, Woods Hole Oceanographic Institute, 18 pp.

McGillis, W. R., Edson, J. B., Ware, J. D., Dacey, J. W. H., Hare, J. E., Fairall, C. W., and Wanninkhof, R.: 1999, 'Carbon Dioxide Flux Techniques Performed during GasEx98', *J. Marine Chem.*, in revision.

Mestayer, P. G. and Rebattet, C.: 1985, 'Temperature Sensitivity of Lyman-Alpha Hygrometers', *J. Atmos. Oceanic Tech.* **2**, 20–25.

Monahan, E. C. and Torgeresen, T.: 1991, 'The Enhancement of Air–Sea has Exchange by Oceanic Whitecapping', in S. C. Wilhelms and J. S. Gulliver (eds.), *Air–Water Mass Transfer: Proceedings of the 2nd International Symposium on Gas Transfer at Water Surfaces*, American Society of Civil Engineers, New York, pp. 608–617.

Ocampo-Torres, F.J. and Donelan, M. A.: 1994, 'Laboratory Measurements of Mass Transfer of Carbon Dioxide and Water Vapour for Smooth and Rough Flow Conditions', *Tellus* **46B**, 16–32.

Ohtaki, E. and Matsui, T.: 1982, 'Infrared Device for Simultaneous Measurement of Fluctuations of Atmospheric Carbon Dioxide and Water Vapor', *Boundary-Layer Meteorol.* **24**, 109–119.

O'Muircheartaigh, I. and Monahan, E. C.: 1986, 'Statistical Aspects of the Relationship between Oceanic Whitecap Coverage, Wind Speed, and Other Environmental Factors', in E. C. Monahan and G. M. Niocaill (eds.), *Oceanic Whitecaps*, D. Reidel, Dordrecht, pp. 125–128.

Oncley, S. P., Delaney, A. C., and Horst, T. W.: 1993, 'Verification of Flux Measurement Using Relaxed Eddy Accumulation', *Atmos. Environ.* **27A**, 2417–2426.

Oost, W.: 1995, 'The ASGASEX'93 Experiment', in B. Jahne and E. C. Monahan (eds.), *Air–Water Gas Transfer*, AEON Verlag & Studio, Hanau, Germany, pp. 811–816.

Oost, W.: 1998, *The ASGAMAGE Workshop*, Report 98-02, KNMI, De Bilt, the Netherlands, 126 pp.

Oost, W. A., Fairall, C. W., Edson, J. B., Smith, S. D., Anderson, R. J., Wills, J. A. B., Katsaros, K. B., and DeCosmo, J.: 1994, 'Flow Distortion Calculations and their Application in HEXMAX', *J. Atmos. Ocean. Technol.* **11**, 366–386.

Panofsky, H. A.: 1963, 'Determination of Stress from Wind and Temperature Measurements', *Quart. J. Roy. Meteorol. Soc*, **89**, 85–94.

Panofsky, H. A. and Dutton, J. A.: 1984, *Atmospheric Turbulence*, Wiley-Interscience, New York, 397 pp.

Paulson, C. A.: 1970, 'The Mathematical Representation of Wind Speed and Temperature Profiles in the Unstable Atmospheric Surface Layer', *J. Appl. Meteorol.* **9**, 857–861.

Rannik, U., Vesala, T., and Keskinen, R.: 1997, 'On the Damping of Temperature Fluctuations in a Circular Tube Relevant to the Eddy Covariance Measurement Technique', *J. Geophys. Res.* **102**, 12789–12794.

Reichardt, H.: 1951, 'Vollstandige Darstellung der turbulenten Geschwindigkeitsverteilung in glatten Leitungen', *Z. Angew. Math. Mech.* **31**, 208–219.

Schmitt, K. F., Friehe, C. A., and Gibson, C. H.: 1978, 'Humidity Sensitivity of Atmospheric Temperature Sensors by Salt Contamination', *J. Phys. Oceanog.* **8**, 141–161.

Simpson, I. J., Edwards, G. C., Thurtell, G. W., denHartog, G., Neumann, H. H., and Staebler, R. M.: 1997, 'Micrometeorological Measurements of Methane and Nitrous Oxide Exchange above a Boreal Aspen Forste', *J. Geophys. Res.* **102**, 29331–29341.

Smith, S. D.: 1988, 'Coefficients for Sea Surface Wind Stress, Heat Flux, and Wind Profiles as a Function of Wind Speed and Temperature', *J. Geophys. Res.* **93**, 15,467–15,472.

Smith, S. D. and Jones, E. P.: 1985, 'Evidence for Wind-Pumping of Air–Sea Gas Exchange Based on Direct Measurements of CO_2 Fluxes', *J. Geophys. Res.* **90**, 869–875.

Smith, S. D. and Jones, E. P.: 1986, 'Isotopic and Micrometeorological Ocean CO_2 Fluxes: Different Time and Space Scales', *J. Geophys. Res.* **91**, 10529–10532.

Smith, S. D., Anderson, R. J., Jones, E. P., Desjardins, R. L., Moore, R. M., Hertzman, O., and Johnson, B. D.: 1991, 'A New Measurement of CO_2 Eddy Flux in the Nearshore Amtospheric Surface Layer', *J. Geophys. Res.* **96**, 8881–8887.

Smith, S. D., Fairall, C. W., Geernaert, G. L., and Hasse, L.: 1996, 'Air–Sea Fluxes: 25 Years of Progress', *Boundary-Layer Meteorol.* **78**, 247–290.

Soloviev, A. V. and Schluessel, P.: 1994, 'Parameterization of the Cool-Skin of the Ocean and of the Air–Ocean Transfer on the Basis of Modeling Surface Renewal', *J. Phys. Oceanog.* **24**, 1377–1416.

Terray, E. A., Donelan, M. A., Agrawal, Y. C., Drennan, W. M., Kahma, K. K. A. J., Williams, I., Hwang, P. A., and Kitaigorodskii, S. A.: 1996, 'Estimates of Kinetic Energy Dissipation under Breaking Waves', *J. Phys. Oceanog.* **26**, 792–807.

Toba, Y.: 1965, 'On the Giant Sea-Salt Particles in the Atmosphere. II – Theory of the Vertical Distribution in the 10-m Layer over the Ocean', *Tellus* **17**, 365–382.

Tong, C., Wyngaard, J. C., Khanna, S., and Brasseur, J. G.: 1998, 'Resolvable- and Subgrid-Scale Measurements in the Atmospheric Surface Layer: Techniques and Issues', *J. Atmos. Sci.* **55**, 3114–3126.

Vickers, D. and Esbensen, S. K.: 1998, 'Subgrid Surface Fluxes in Fair Weather Conditions during TOGA COARE: Observational Estimates and Parameterization', *Mon. Wea. Rev.* **126**, 620–633.

Wanninkhof, R.: 1992, 'Relationship Between Wind Speed and Gas Exchange over the Ocean', *J. Geophys. Res.* **97**, 7373–7382.

Weare, B. C. and Strub, P. T.: 1982, 'The Significance of Sampling Biases on Calculated Monthly Mean Oceanic Surface Heat Fluxes', *Tellus* **33**, 211–224.

Webb, E. K., Pearman, G. I., and Leuning, R.: 1980, 'Correction of Flux Measurements for Density Effects Due To Heat and Vapor Transfer', *Quart. J. Roy. Meteorol. Soc.* **106**, 85–100.

Wesely, M. L.: 1986, 'Response to "Isotopic Versus Micrometeorologic Ocean CO_2 Fluxes: A Serious Conflict", by W. Broecker et al.', *J. Geophys. Res.* **91**, 10533–10535.

Wesely, M. L., Cook, D. R., Hart, R. L., and Williams, R. M.: 1982, 'Air–Sea Exchange of CO_2 and Evidence for Enhanced Upward Fluxes', *J. Geophys. Res.* **87**, 8827–8832.

Woolf, D. K.: 1997, 'Bubbles and their Role in Gas Exchange', in R. A. Duce and P. S. Liss (eds.), *The Sea Surface and Global Change*, Cambridge University Press, New York, NY, pp. 173–205.

Wyngaard, J. C.: 1973, 'On Surface-Layer Turbulence', in D. A. Haugen (ed.), *Workshop on Micrometeorology*, Amer. Meteorol. Soc., pp. 101–149.

Wyngaard, J. C.: 1990, 'Scalar Fluxes in the Planetary Boundary Layer – Theory, Modeling, and Measurement', *Boundary-Layer Meteorol.* **50**, 49–75.

Wyngaard, J. C., Izumi, I., and Collins, S. A.: 1971, 'Behavior of the Refractive Index Structure Parameter near the Ground', *J. Opt. Soc. Amer.* **61**, 1646–1650.

Yelland, M. J., Taylor, P. K., Consterdine, I. E., and Smith, M. H.: 1994, 'The Use of the Inertial Dissipation Technique for Shipboard Wind Stress Determination', *J. Atmos. Ocean. Technol.* **11**, 1093–1108.

Zeng, X., Zhao, M., and Dickinson, R. E.: 1998, 'Comparison of Bulk Aerodynamic Algorithms for the Computation of Sea Surface Fluxes Using the TOGA COARE Data', *J. Clim.* **11**, 2628–2644.

Zulauf, M. and Krueger, S. K.: 1997, 'Parameterization of Mesoscale Enhancement of Large-Scale Surface Flxues over Tropical Oceans', in *Proceedings of the 12th Symposium on Boundary Layers and Turbulence*, American Meteorological Society, 28 July–1 August, Vancouver, BC, Canada, 1997, pp. 494–495.